CONTROL-ORIENTED ANALYSIS OF AEROTHERMOELASTIC EFFECTS FOR A HYPERSONIC VEHICLE

By

SANKETH BHAT

A THESIS PRESENTED TO THE GRADUATE SCHOOL
OF THE UNIVERSITY OF FLORIDA IN PARTIAL FULFILLMENT
OF THE REQUIREMENTS FOR THE DEGREE OF
MASTER OF SCIENCE

UNIVERSITY OF FLORIDA

2008

"Sarva mangala mangalye sive sarvardha sadhike

saranye trayambake gauri narayani namostute"

Dedicated with love to my parents and to my brother.

ACKNOWLEDGMENTS

I would like to acknowledge the management at NASA because none of this work would have been possible without their support. I would also like to extend my sincere thanks to Dr. Warren Dixon and Dr. Anil Rao for agreeing to be on my committee. Heartfelt thanks go out to the senior researchers at the Flight Control Lab, including Dr. Joe Kehoe, Dr. Ryan Causey, Dr. Mujahid Abdulrahim, Dr. Adam Watkins, and Dr. Sean Regisford for their valuable guidance and support. This effort would not have been possible without the help of my fellow researchers at the Flight Control Lab, including Brian Roberts, Robert Love, Baron Johnson, Ryan Hurley, Dong Tran and of course, my desk buddy, Daniel *Tex* Grant, for lighting up many a days with his humor. I would like to express my sincere and deep gratitude to Dr. Rick Lind for his guidance, support, and most importantly for giving me this opportunity to prove myself. My parents and my brother deserve much credit for making me what I am and showing me the right way all these years. I thank all who helped me get this far, but whose names I inadvertently missed out.

TABLE OF CONTENTS

LIST OF TABLES

LIST OF FIGURES

Abstract of Thesis Presented to the Graduate School
of the University of Florida in Partial Fulfillment of the
Requirements for the Degree of Master of Science

CONTROL-ORIENTED ANALYSIS OF AEROTHERMOELASTIC EFFECTS FOR A HYPERSONIC VEHICLE

By

Sanketh Bhat

December 2008

Chair: Richard C. Lind, Jr.
Major: Aerospace Engineering

Hypersonic flight is seen as a feasible solution to make space travel faster, safer and more affordable. The design of the Air-breathing hypersonic vehicle is such that there is coupling between the structure and the propulsion system. Therefore, the aerodynamic, propulsion and the structural effects must be accounted to effectively model the vehicle. The vibrations from the structure affect the performance of the vehicle. Hence, vibration attenuation is a critical requirement for hypersonic vehicles. The problems of vibration are compounded by variations in heating during flight. Structural variations resulting from the tremendous heating incurred during hypersonic fight is mitigated by a thermal protection system (TPS); however, such mitigation is accompanied by an increase in weight that can be prohibitive. The actual design of a thermal protection system can be chosen to vary the level of heating reduction, and associated weight, across the structure.

Our study examined the design of a Linear Parameter Varying controller for an hypersonic vehicle and describes the process of control-oriented analysis to suggest a better 'Thermal Protection System' for the vehicle. A Linear Parameter Varying control architecture was used that damps any thermal effects for a range of temperature profiles. Various designs are considered for a representative model to show the large variation in flight dynamics. Simulation results indicate that the proposed methodology may constitute a feasible approach toward the development of a robust Linear Parameter Varying controller to satisfactorily address the issue of temperature effects on the dynamics of the

vehicle. From the above closed-loop design analysis, important information regarding the open-loop dynamics can be obtained. We then considered how such designs and resulting thermal gradients influence the ability to achieve closed-loop performance. The resulting closed-loop performance is characterized as a function of the induced thermal gradients to indicate the optimality of the design. It is also shown that the introduction of control synthesis merely adds a linear dependency onto a nonlinear dependency which does not overly increase the computational challenge.

CHAPTER 1
INTRODUCTION

1.1 Motivation

Humans are on a quest to move faster and higher. Commercial groups want a more reliable way of putting payload in the low earth orbit. Defense organizations want a high speed and high altitude bomber. Air-breathing hypersonic vehicles (HSV) are seen as a feasible solution to make space travel affordable and safe. Hypersonic flight is being aggressively pursued as a capability to traverse the world in a few hours. A class of vehicles under consideration utilize a design in which a wedge-shaped fuselage provides lift and acts as an inlet for the SCRAMjet engine. This configuration and its associated aeropropulsive characteristics was successfully demonstrated on the X-43 prototype. The vehicle (Figure 1-1), has a tightly integrated airframe and SCRAMjet propulsion system (1).

Figure 1-1. Air-breathing hypersonic vehicle

The design of hypersonic vehicles is maturing with respect to the aeropropulsive interactions of the fuselage and engine; however, the aerothermoelastic characteristics must also be addressed. Vibration attenuation is a critical requirement for these vehicles

because any displacement of the fuselage will affect the engine performance. The control challenge is compounded by temperature effects that significantly alter the structural dynamics throughout the flight as the fuselage heats.

A novel approach to control the hypersonic vehicle, namely a multi-loop architecture is formulated that contains compensators for vibration suppression, maneuvering and engine control. This architecture directly matches a modeling scheme for the open-loop dynamics that couples aerodynamics and structural dynamics with engine dynamics. The inner-loop controller is used to actively augment damping of the structural modes. The outer-loop controller is then used to achieve rigid-body performance specifications. Finally, an engine controller operates continuously to guarantee proper propulsion despite variations in the flight dynamics. Also, the architecture includes both gain-scheduled elements and adaptive elements. The gain-scheduled elements represent pre-flight designs using high-fidelity models whereas the adaptive elements are used to cancel any residual errors. Essentially, the adaptive elements only affect the system when aerothermoelastic dynamics vary beyond theoretical ranges and the gain-scheduled controller is unable to achieve the desired performance of either the flight path or engine propulsion.

This study, however restricts consideration only to the inner-loop LPV controller. This analysis also introduces a control-oriented design for hypersonic vehicles that directly considers mission capability. In this case, the design seeks to choose a thermal protection system (TPS) and associated controller that maximize vibration attenuation.

1.2 Overview

A typical mission for this vehicle is to place a payload into low Earth orbit which requires the vehicle to operate in many flight regimes such as subsonic, transonic, supersonic, hypersonic and orbital. However, this study limits consideration to the hypersonic regime while still in the atmosphere. The ground vibration test (GVT) system is necessary to assure the aeroelastic and aeroservoelastic stability of new and modified aerospace vehicle. The hypersonic vehicle, shown during ground vibration test

(Figure 1-2), demonstrated the suitability of a SCRAMjet engine in this configuration for hypersonic flight.

Figure 1-2. The X-43 model during GVT

There have been several papers in literature that have discussed challenges associated with the dynamics and control of hypersonic vehicles. A detailed analytical model of the longitudinal dynamics was undertaken by Chavez and Schmidt (2). A slightly different approach to develop the model was undertaken by Bolender and Doman (1; 3; 4) which is further developed by the same authors (5; 6). Another model of the hypersonic vehicle was developed using piston theory (7). Using the above models as a fixed design, several approaches for control have been considered including H_∞ (8), μ synthesis (9) and Linear Parameter Varying (LPV) control (10). Additional work has even considered sensor placement (11–15). A CFD approach to develop a model of hypersonic vehicle is presented in (16). Various control strategies for the hypersonic vehicle like adaptive control (17–20) and other linear control theories (21–23) have been discussed in literature.

The dynamics of air-breathing hypersonic vehicles include couplings between the engine and flight dynamics, in addition to the interactions between flexible and rigid

body modes. (24) discusses the development of a control-oriented model in closed form by replacing complex force and moment functions with curve-fitted approximations, neglecting certain weak couplings, and neglecting slower portions of the system dynamics. The advantage of this approach is that the linear control strategies need not be used, but the modeling process is time-consuming.

For the control design, there are several issues that must be addressed. The controller must account for strongly coupled aerodynamics-propulsion dynamics and actively suppress modal vibrations. Aerothermoelastic effects cannot be ignored in a hypersonic flight and must be compensated. The choice of control architecture is closely related to the previous issues. Generating a single state-space controller that provides stability and performance seems somewhat limited because it may be advantageous to link certain parts of the controller to certain dynamics of the model. Also, the theories involving H_∞ and μ synthesis only considered a single flight condition.

Investigations into aerothermoelastic design are not as mature because of the challenges associated with simultaneous optimization of both the structure and the controller. Many previous efforts into the general problem of structure-control design have noted its inherent nonlinearities that can be solved using a variety of formulations including linear matrix inequalities and bi-linear matrix inequalities (25–28).

The control-oriented design is optimized using a parametrized solution to a Riccati equation. System design is intractable when trying to optimize both open-loop dynamics and feedback compensator simultaneously; alternatively, system design is actually manageable when trying to optimize the open-loop dynamics with respect to a feasibility condition that guarantees the existence of a feedback compensator. In this way, the actual controller does not need to be computed but merely an open-loop design for which a controller is guaranteed to exist will be designed.

This concept of control-oriented design represents a significant advancement to the state-of-the-art for the community and is particularly advantageous for next-generation

vehicles. Traditional approaches, which are satisfactory for traditional vehicles, will not be able to maximize mission capability for future classes of vehicles that will operate at off-cruise conditions, utilize high agility, include time-varying dynamics, and require complex interactions among the dynamics.

CHAPTER 2
CONTROL DESIGN

2.1 Vehicle

The hypersonic model (5) used in our study, is limited to longitudinal motion and is developed with eleven states, four inputs and eleven outputs. The states include five rigid body states, velocity (V), angle of attack (α), pitch rate (Q), altitude (h), pitch attitude (θ) and six elastic states for the first three fuselage bending modes ($\eta_i, \dot{\eta}_i$). The inputs include elevator deflection (δ_e), canard deflection (δ_c), diffuser area ratio (A_d) and fuel flow ratio (Φ). The model has full state feedback i.e. all the eleven states are used as feedback to the controller. Aerodynamic, inertial, propulsive, and elastic forces were used to derive the equations of motion for the hypersonic vehicle (1).

To incorporate structural dynamics and aerothermoelastic effects in the hypersonic vehicle dynamic model, an assumed modes model is considered for the longitudinal dynamics (5) as,

$$
\begin{aligned}
\dot{\mathrm{V}} &= \tfrac{\mathrm{T}\cos(\alpha)-\mathrm{D}}{m} - \mathrm{g}\sin(\theta-\alpha) \\
\dot{\mathrm{h}} &= \mathrm{V}\sin(\theta-\alpha) \\
\dot{\alpha} &= -\tfrac{\mathrm{L}+\mathrm{T}\sin(\alpha)}{\mathrm{mV}} + \mathrm{Q} + \tfrac{\mathrm{g}}{\mathrm{V}}\cos(\theta-\alpha) \\
\dot{\theta} &= \mathrm{Q} \\
\dot{\mathrm{Q}} &= \tfrac{\mathrm{M}}{\mathrm{Iyy}} \\
\ddot{\eta}_i &= 2\varsigma_i\omega_i\dot{\eta}_i - \omega_i^2\eta_i + N_i, i = 1,2,3
\end{aligned}
$$

$m \in \mathbb{R}$ denotes the vehicle mass, $I_{yy} \in \mathbb{R}$ is the moment of inertia, g $\in \mathbb{R}$ is the acceleration due to gravity, T(t) $\in \mathbb{R}$ denotes thrust, D(t) $\in \mathbb{R}$ denotes drag, L(t) $\in \mathbb{R}$ is lift, $\xi_i, \omega_i \in \mathbb{R}$ are the damping factor and natural frequency of the i^{th} flexible mode, respectively, and $N_i \in \mathbb{R}$ denote generalized elastic forces. The equations that define the aerodynamic and generalized moments and forces are lengthy and are omitted for brevity. Details of the moments and forces are provided in (1). Because of aerothermolelastic

interactions, the temperature profile of the hypersonic vehicle will vary in time. As the temperature profile changes, the damping factors and natural frequencies of the flexible modes will change.

2.2 Aerothermoelasticity

Aerothermoelasticity can be said to be the response of elastic structures to aerodynamic heating and loading. In recent years, the focus in the area of hypersonic aeroelasticity and aerothermoelasticity has been predominantly on the development of computational aeroelastic and aerothermoelastic methods capable of studying complete hypersonic vehicles (29–37).

It has been shown in literature that the exact computation of the thermal effects on the aerodynamics of an aerospace craft in the hypersonic regime is difficult (38). Hence, this study concentrates only on the effects of aerothermoelasticity. The way this is done is by noting the variations in the structural properties as a function of temperature.

The hypersonic vehicle is subjected to extreme temperatures and heating during the hypersonic flight regime. Hence, the structure needs to be protected by a Thermal Protection System (TPS). To study the temperature effects, various temperature gradients along the fuselage of the vehicle are introduced into the model simulating the temperatures attained by the vehicle in flight. Knowing the material properties such as Young's modulus (E) (39) as a function of temperature, the effects on the structural properties like the mode shapes, natural frequencies and damping are analyzed. For example, the variations in the representative mode shapes for a beam at different temperatures can be analyzed to study the effect of temperature on the dynamics (Figure 2-1). In this case, the bending mode is extracted to indicate changes such as node location, anti-node location, and magnitude of oscillation. This behavior is incorporated into flight models through aerothermoelastic dynamics.

It has been impressed before that to represent the dynamics of the vehicle accurately, the model must be formulated to include the effects of structural flexibility in addition

Figure 2-1. Mode shapes with thermal variation

to the dynamics of the rigid-body. This section describes the formulation of a state-space model that includes rigid-body and structural dynamics. The model structure developed here is based on the work of (40–42). The general form of the state-space model is (43):

$$\dot{x} = Ax + Bu$$

where, x is the vector of states, u is the vector of control inputs, A is the stability matrix and B is the matrix of control inputs.

With the structural effects included, A and B are of the form,

$$A = \begin{bmatrix} \text{RigidBody} & \text{Aeroelastic} \\ \text{Terms} & \text{CouplingTerms} \\ \\ \text{RigidBody} & \text{Structural} \\ \text{CouplingTerms} & \text{FlexibilityTerms} \end{bmatrix}$$

$$B = \begin{bmatrix} \text{RigidBodyControl} \\ \text{StructuralModeControl} \end{bmatrix}$$

where the 'Rigid Body Terms' are the rigid-body portions of the model, the 'Structural Flexibility Terms' are the dynamics of the structural modes included in the model, and the

'Aeroelastic Couping Terms' and 'Rigid Body Coupling Terms' are the coupling between the rigid-body and the structural flexibility of the vehicle.

The aerothermoelastic effects during a typical flight profile were studied for the National Aerospace Plane (NASP) (44). This study noted that the surface temperatures could range from 0^oF to nearly 5000^oF at certain points and result in large surface gradients. Consequently, the natural frequencies and damping of the structural modes can vary significantly by up to 30%. These effects will be used as representative effects that may be encountered for the general class of vehicles considered in this study.

The aerothermoelastic effects were noted to cause a decrease in natural frequency and damping of the structural modes. This effect is incorporated by formulating the state matrix as an affine function of temperature. The range of temperatures considered for this model is chosen as $\theta \in (0^oF, 1000^oF)$ to match the operating range of Titanium (Ti).

2.3 Linear Parameter Varying

2.3.1 Framework

Gain Scheduling is said to be a linear regulation of the system whose parameters are functions of the operating conditions. It is basically a 'divide and conquer' control strategy where the operating conditions are broken down into linear sub-problems (45). The three main classes of aerospace systems using the concept of gain scheduling are Linear Time Invariant (LTI), Linear Time Varying (LTV) and Linear Parameter Varying (LPV).

Gain Scheduling can be broken down into three steps (46). Firstly, separate the operating range into subspaces and create parameterized model for each subspace. Then, create controllers for each of the models and then develop a scheduling scheme by linearly interpolating between these regional controllers for the local subspaces. However, there is no guarantee of stability and robustness with respect to uncertainties in the dynamics and there is a possibility of skipping behavior during switch between controllers. Also, developing the linear interpolation law can be rigorous and time consuming.

The theory of LPV offsets some of the disadvantages of gain scheduling. The LPV framework develops one controller over the entire operating range and guarantees robustness and stability. In the LPV framework, the plant model must be created as a linear parameter varying system.

Robust identification techniques for special classes of LPV systems are presented in (47; 48). A method of identifying multi-variable LPV state space systems that are based on local parameterization and gradient search in the resulting parameter space is presented in (49). Two identification methods were proposed in (50) for a class of multi-input multi-output discrete time linear parameter varying systems. Both methods are based on the subspace state space method, which was suggested by (51). (52) suggests two methods for modeling aircraft dynamics, namely, the bounding box and small hull approach. Another approach to solve the LPV systems which are characterized by a set of linear matrix inequalities (LMI) is presented in (53).

A typical case of a linear parameter varying plant $P(.,\theta)$, whose dynamical equations depend on physical coefficients that vary during operation, has the form

$$P(.,\theta) = \begin{cases} \dot{x} = A(\theta)x + B_1(\theta)d + B_2(\theta)u \\ e = C_1(\theta)x + D_{11}(\theta)d + D_{12}(\theta)u \\ y = C_2(\theta)x + D_{21}(\theta)d + D_{22}(\theta)u \end{cases} \tag{2–1}$$

where

$$\theta\,(t) = (\theta_1(t), ..., \theta_n(t)), \underline{\theta}_i \leq \theta_i(t) \leq \overline{\theta}_i \tag{2–2}$$

is a time varying vector of physical parameters, for example, velocity, angle of attack, temperature; A, B, C, D are affine functions of $\theta(t)$, x is the state vector, y is the measured output, e is the regulated output or errors, d is the exogenous disturbances, and u is the regulated input.

2.3.2 Synthesis

If the parameter vector $\theta(t)$ takes values within the geometric shape of $\mathbf{R}^n$ with corners $\{\Pi_i\}_{i=1}^N$ $(N = 2n)$, the plant system matrix (46)

$$S(\theta) := \begin{bmatrix} \dot{x} \\ e \\ y \end{bmatrix} = \begin{bmatrix} A(\theta(t)) & B(\theta(t)) \\ C(\theta(t)) & D(\theta(t)) \end{bmatrix} \begin{bmatrix} x \\ d \\ e \end{bmatrix} \tag{2–3}$$

ranges in a matrix polytope with vertices $S(\Pi_i)$. Given a convex decomposition,

$$\theta(t) = \alpha_1\Pi_1 + ... + \alpha_N\Pi_N, \quad \alpha_i \geq 0, \quad \sum_{i=1}^{N} \alpha_i = 1 \tag{2–4}$$

of θ over the corners of the parameter region, the system matrix is given by

$$S(\theta) = \alpha_1 S(\Pi_1) + ... + \alpha_N S(\Pi_N) \tag{2–5}$$

This suggests seeking a parameter dependent controllers with equations

$$K(.,\theta) \begin{cases} \dot{\xi} = A_K(\theta)\xi + B_K(\theta)y \\ u = C_K(\theta)\xi + D_K(\theta)y \end{cases} \tag{2–6}$$

and with a vertex property where a given convex decomposition $\theta(t) = \sum_{i=N}^{n} \alpha_i\Pi_i$ of the current parameter value $\theta(t)$. The controller state-space matrices at the operating point $\theta(t)$ are obtained by convex interpolation of the LTI vertex controllers

$$K_i := \begin{pmatrix} A_K(\Pi_i) & B_K(\Pi_i) \\ C_K(\Pi_i) & D_K(\Pi_i) \end{pmatrix} \tag{2–7}$$

This yields a smooth scheduling scheme of the controller matrices by the parameter measurements $\theta(t)$.

There are many techniques to make the LPV controller once the system has been put in the LPV framework. The three main synthesis techniques are μ synthesis design

(54), Linear Quadratic Gaussian (LQG) design (55), and H_∞ (56). In this study, the H_∞ technique has been used and the control problem can be formulated as 'linear matrix inequalities' (LMI), which as shown in (57) is a convex optimization problem. (58) has an example of creating a convex optimization problem with LMI expressions for the use of finding an LPV controller for the attitude control of an X-33.

CHAPTER 3
CONTROL-ORIENTED DESIGN

3.1 Closed-Loop Design Space

Systems are evaluated on their ability to perform missions; consequently, the design space must include all parameters that affect such ability. The design space can be said to be the n-dimensional region over which the objective and constraints are defined where n is the number of independent design variables. The closed-loop operation of such systems suggests a decomposition of the design into separate subspaces. This decomposition follows the generalized block diagram, (Figure 3-1), as a feedback relationship between the open-loop plant and a controller. In the diagram, d is the vector of exogenous inputs or disturbances including reference commands and e is the vector of errors to be minimized. There have been on-going studies to develop algorithms for optimizing the design space for

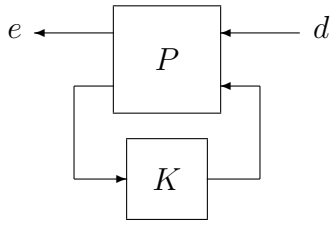

Figure 3-1. Closed-loop block diagram

aerospace systems. Most optimization designs start with the fixed design space. But, since the feasible region in the fixed space is very small and the probability of finding a proper solution is low, (60) proposes a probabilistic approach for the feasibility improvement of the design space. (61) presents a novel hybrid optimization method to efficiently find the global optimal of complex, highly multi modal systems. (62) proposes a methodology for the analysis and design of systems subject to parametric uncertainty in which design requirements are specified via hard inequality constraints. Hard constraints are those that must be satisfied for all parameter realizations within a given uncertainty model.

A design space is formulated using the parameters that affect the open-loop dynamics. This space, defined as $\mathbb{P}$, can include a wide variety of parameters including geometry,

structure, materials and other aspects related to vehicle design. A particular configuration of the open-loop dynamics is thus represented by the vector, $\pi \in \mathbb{P}$, within the design space.

Another design space is formulated that contains the compensator elements that may be varied. This space, defined as $\mathbb{K}$, can include aspects of the feedback compensator such as gains, lags, bandwidth, and adaption rates along with sensors and actuators. Any controller is thus formulated using the vector, $\kappa \in \mathbb{K}$, from within the design space.

The set of closed-loop systems that are possible candidates for the optimal configuration can be represented by $\mathbb{T}$. This set notes that the open-loop plant, $P(\pi)$, depends on the design space of $\mathbb{P}$ and the compensator, $K(\kappa)$, depends on the design space of $\mathbb{K}$. Finally, the set of all closed-loop systems $\mathbb{T}$ can be described as a Linear Fractional Transformation (LFT),

$$\mathbb{T} = \{F_l\left(P(\pi), K(\kappa)\right) \;\; \pi \in \mathbb{P}, \kappa \in \mathbb{K}\}$$

Also, the set of $\mathbb{T}$ can utilize a standard reduced-order model of the open-loop dynamics. Standard tools can compute state-space models using high-fidelity approaches from computational fluid dynamics or computational structural dynamics. A basic representation of a state-space model, $P = \{A, B, C, D\}$, is introduced although other representations can easily be substituted into the approach

$$\mathbb{T} = \{F_l\left(\{A(\pi), B(\pi), C, D\}, K(\kappa)\right) \;\; \pi \in \mathbb{P}, \kappa \in \mathbb{K}\}$$

3.2 Feasibility-Based Optimization

In mathematics, H_∞ is the space of matrix-valued functions that are analytic and bounded in the open right-half of the complex plane defined by Re(s) > 0. The H_∞ norm is the maximum singular value of the function over that space. This can be interpreted as a maximum gain in any direction and at any frequency. For example, in SISO systems, this is effectively the peak of the magnitude of the frequency response. H_∞ techniques can be used to minimize the closed loop impact of a perturbation, depending on the problem

formulation, the impact will either be measured in terms of stabilization or performance. H_∞ norm can be seen as a gain, so the problem can be reformulated as 'minimize the gain from disturbances to error'.

The metric for design can be cast as an $\mathcal{H}_\infty$-norm condition on the closed-loop system. As such, the design seeks to find the optimal values for both the open-loop dynamics and an $\mathcal{H}_\infty$-norm controller. The computation for that controller is actually somewhat mature using a state-space solution although the joint computation of both dynamics and controller is intractable.

The optimal design actually does not need to compute both the open-loop dynamics and controller simultaneously; instead, the design can simply find the open-loop dynamics for which a controller exists that achieves the lowest $\mathcal{H}_\infty$-norm value.

The synthesis of controllers using modern techniques actually follows a two-step procedure. The initial step iterates over a feasibility check that indicates if a controller exists to achieve a particular value of closed-loop performance. The final step computes the gain for the feedback compensator that achieves the optimal closed-loop performance. This two-step procedure is implemented in professional software such as MATLAB, because a set of feasibility conditions is significantly less computationally expensive than a set of synthesis conditions.

The approach for control-oriented design is now expressed as minimizing the closed-loop norm (γ) with respect to the design space while maintaining the feasibility constraints,

$$\begin{aligned} &\min && \gamma \\ &\pi \in \mathbb{P} \\ &X = X^* > 0 \\ &Y = Y^* > 0 \end{aligned}$$

subject to

$$\begin{aligned} 0 &= XA(\pi) + A(\pi)^* X \\ &\quad + X(\frac{1}{\gamma^2} B_1(\pi) B_1(\pi)^* - B_2(\pi) B_2(\pi)^*) X \\ &\quad + C_1(\pi) * C_1(\pi) \\ 0 &= A(\pi) Y + Y A(\pi)^* \\ &\quad + Y(\frac{1}{\gamma^2} C_1(\pi)^* C_1(\pi) - C_2(\pi)^* C_2(\pi)) Y \\ &\quad + B_1(\pi) B_1(\pi)^* \\ \gamma^2 &> \rho(XY) \end{aligned}$$

where ρ is the spectral radius. This constrained optimization requires finding a minimum to a nonlinear function. The operators of X and Y, if they exist, can be found for any fixed value of π using standard algorithms; however, they are almost certain to have non-convex dependencies when considering all $\pi \in \mathbb{P}$. A variety of numerical approaches can be applied to the minimization including branch and bound, simulated annealing, neural networks, and so on.

Finally, the actual controller that achieves the optimal closed-loop system is computed using the solutions, X and Y, to these Riccati equations. The standard synthesis for $\mathcal{H}_\infty$-norm control is used.

CHAPTER 4
EXAMPLE

4.1 Objective

The mission objective is simply a prescribed change to airspeed and altitude; however, several difficulties must be circumvented for this basic maneuver. The propulsion system is tightly coupled to the fuselage so structural vibrations can cause loss of engine performance. The vibrations are compounded by the introduction of thermal gradients which result from the tremendous heating across the fuselage throughout flight. As such, vibration attenuation becomes a critical aspect of mission performance.

This example represents a single element within a larger multi-loop architecture (38). The fundamental concept uses a pair of loops such that the inner-loop controller provides vibration attenuation while the outer-loop controller provides maneuvering. Such a loop decomposition recognizes that thermal effects are predominantly limited to the structural dynamics related to vibration. The outer-loop controller is thus designed without consideration of temperature effects since the inner-loop controller is assumed to provide adequate compensation.

A baseline vehicle is adopted from an extensive program by the U.S. Air Force for a reduced-order model (1; 3–7). This model includes five states for the rigid-body flight dynamics and an additional six states associated with three flexible-body structural dynamics. The model is particularly attractive in that it contains a rigorous derivation of the aerothermoelastic coupling that explicitly highlights the effects of vibrations on mission performance.

This study can be put into two categories. The first part involves the design of the inner-loop controller using Linear Parameter Varying theory. This analysis is done basically as a 'proof-of-concept'. In the second part, control-oriented analysis is performed to give a design which optimizes the performance of the vehicle.

4.2 The LPV Contol Design

4.2.1 Control Issues

As mentioned earlier, a typical mission for this vehicle would be to put a payload into low Earth orbit which would require the vehicle to operate in many flight regimes such as subsonic, transonic, supersonic, hypersonic and orbital. Each regime introduces control problems that must be alleviated for a successful mission. For example, the control surfaces will probably be small so as to minimize heating during hypersonic flight, but this may create difficulties for properly controlling the vehicle at low supersonic speeds. Another potential control problem may arise from the shocks generated by unsteady aerodynamics at transonic flight. Also, the issue of orbit transfers for payload delivery while in space is a control problem for this type of vehicle that introduces issues not usually affecting atmospheric flight. The control problems in every flight regime are important; however, this study will limit consideration to the hypersonic regime while still in the atmosphere.

Several control issues were identified for investigating hypersonic flight through the atmosphere that must be investigated. Firstly, the controller must actively suppress modal vibrations. The aerothermoelastic effects must be compensated. This issue is generally not considered for traditional aircraft but is quite important for hypersonic flight. The degree of heating resulting from hypersonic flight at high dynamic pressure can be tremendous and result in changing material properties such as stiffness. This change is stiffness can have a dramatic effect on closed-loop properties because the controller must account for the low frequency fuselage bending mode and also the changes to those modal dynamics because of aerothermoelastic effects.

Secondly, the choice of a control architecture is closely related to the previous issue. Generating a single state-space controller that provides stability and performance seems somewhat limited because it may be advantageous to link certain parts of the controller to certain dynamics of the model. In particular, vibration suppression is an extremely

difficult task so it seems logical to separate some elements of modal control from the main flight controller to localize some aspects of the aerothermoelastic dynamics. This structured approach allows the designer to make small changes to only a small part of the synthesis model to improve a specific closed-loop performance problem. The controller must include gain-scheduling strategies that are particularly suitable for hypersonic flight.

A linear parameter-varying (LPV) synthesis can be used to formulate the controller. The resulting controller will be automatically gain scheduled over temperature such that the gains are altered to account for the thermal variations in natural frequency and damping of the structural modes. Also, the closed-loop system can be guaranteed to satisfy stability and performance metrics associated with the uncertainty operators.

The model used to design, the inner-loop controller should characterize performance by increasing the damping of the structural modes of the plants. Therefore, a model-following approach is an acceptable synthesis method. This approach would attempt to make the inner-loop system similar to a desired inner-loop system that has acceptable modal damping. Weighting functions can be used to shape the resulting controller such that there is little gains at low and high frequency to ensure the inner-loop controller does not adversely interact with the outer-loop controller.

4.2.2 Modeling Thermal Profile

The effect of temperature variations on the flight dynamics of a hypersonic vehicle need to be analyzed and understood in order to develop an effective control law. The temperature variations have an impact on the structural dynamics as it affects the mode shapes, natural frequencies and the flight dynamics. The natural frequencies of a continuous beam are dependent on the mass distribution of the beam and the stiffness. The stiffness, in turn, is dependent on the Young's Modulus (E) and admissible mode functions. Hence, by modeling the Young's Modulus as a function of temperature, the effect of temperature on the flight dynamics can be captured. Generally, for a given material, the Young's modulus decreases with an increase in temperature.

Different temperature gradients along the fuselage are introduced into the model. This study restricts analysis to decreasing gradients from the nose to the tail as it is expected that the nose will always be the hottest part and the tail will be the coldest part of the structure. The material of the fuselage below the TPS is assumed to be Titanium (4; 6).

Initially, fifteen temperature profiles introduced into the model (Figure 4-1). The first five profiles are linear i.e the temperature gradient linearly decreases from nose to tail, the next five have gradients lesser than the linear profiles and the last five have gradients greater than the linear profiles. The fuselage has been divided into nine equal sections.

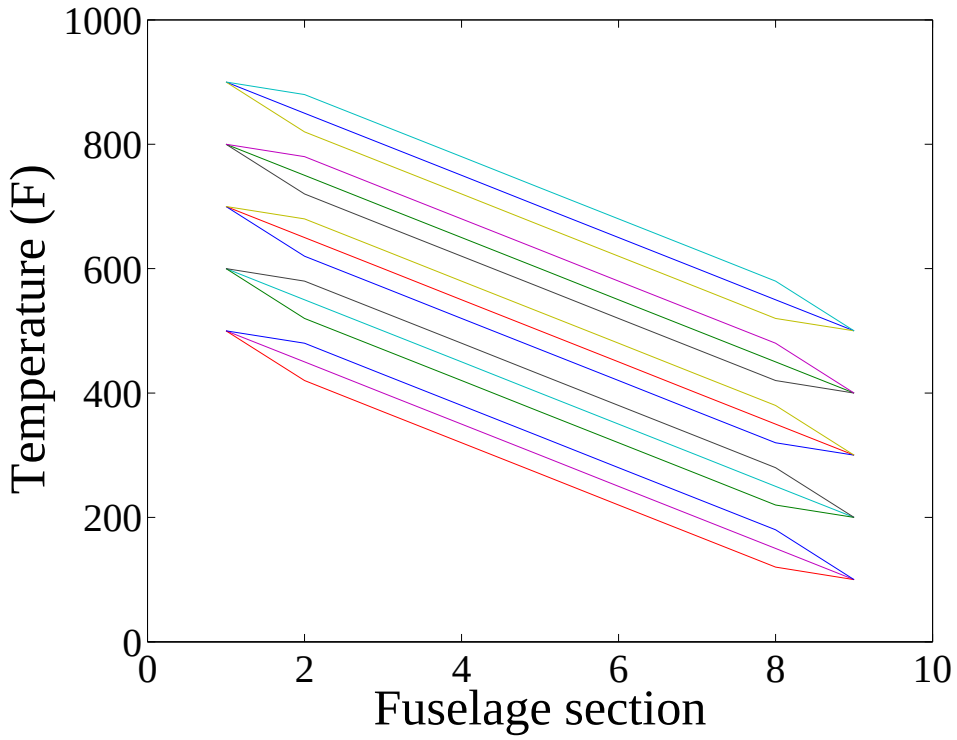

Figure 4-1. Different temperature profiles

The transfer functions from pitch rate to elevator deflection for the different temperature profiles are plotted (Figure 4-2). The first peak represents the unstable rigid body mode. It is observed that there is a variation in both, the damping and the natural frequencies of the structure. It is expected that the natural frequency should

decrease with an increase in temperature. There is about 7% variation in the natural frequencies for the linear temperature profiles (Table 4-1). However, the mode shapes show very little change with temperature (Figure 4-3). The asymmetric nature of the mode shape shows the dependence of the structural properties on the temperature gradients.

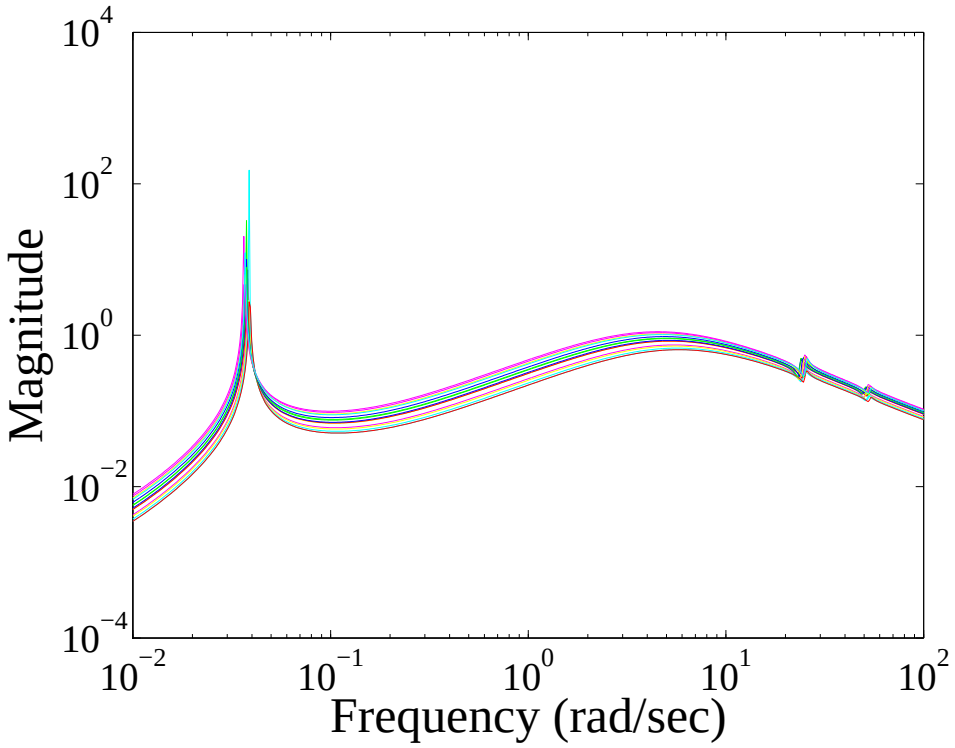

Figure 4-2. Transfer Function from pitch rate to elevator deflection

Table 4-1. Natural frequencies for the linear temperature profiles

Mode	1(*hottest*)	2	3	4	5	Reduction (%)
1	23.01	23.50	23.90	24.31	24.73	6.96
2	49.87	50.89	51.78	52.62	53.54	6.85
3	98.90	100.95	102.7	104.4	106.21	6.88

4.2.3 Flight Dynamics

The plant model corresponding to the linear profile with the nose temperature at $700^{o}F$ and tail temperature at $300^{o}F$ is chosen as the nominal model for this analysis. It is observed that some of the coefficients of the stability matrix, $A(\theta)$ and control matrix,

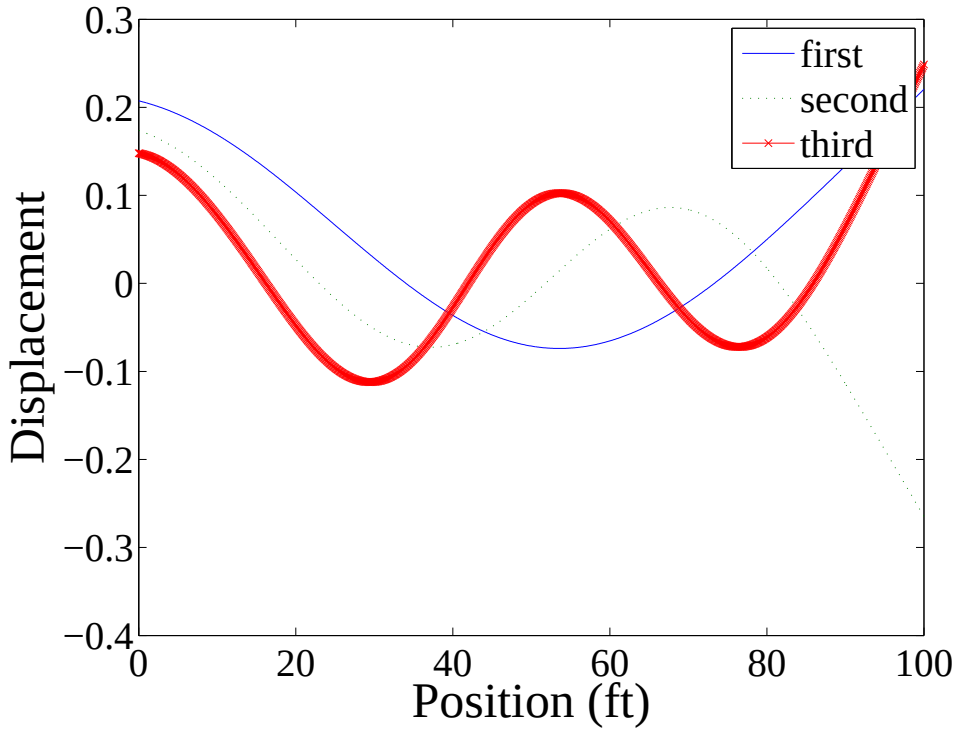

Figure 4-3. Mode shapes for the vehicle

$B(\theta)$ in the state equation,

$$\dot{x}(t) = A(\theta)x(t) + B(\theta)u(t) \tag{4–1}$$

show a strong dependence on temperature.

$A(i,j)$ and $B(i,k)$ represents the effect of the j^{th} state or k^{th} control input on the rate of change of the i^{th} state. The coefficients $A(3,2)$, $A(7,6)$ and $B(3,1)$ show considerable variations with temperature. $A(3,2)$ represents the influence of angle of attack on the pitch rate, $A(7,6)$ represents the influence of the first bending mode displacement on the first bending mode velocity and $B(3,1)$ represents the influence of the elevator deflection on the pitch rate. It is observed that $A(3,2)$ affects only the unstable rigid body mode whereas $A(7,6)$ and $B(3,1)$ affects only the flexible modes. The variation of the coefficients for the different plant models are then analyzed (Figure 4-4). It can be seen $A(7,6)$ decreases with a decrease in temperature, but it is difficult to find a structure in

the other two coefficients. $A(3,2)$ and $B(3,1)$ have a nonlinear and unstructured nature but show a similar trend with respect to the different temperature profiles.

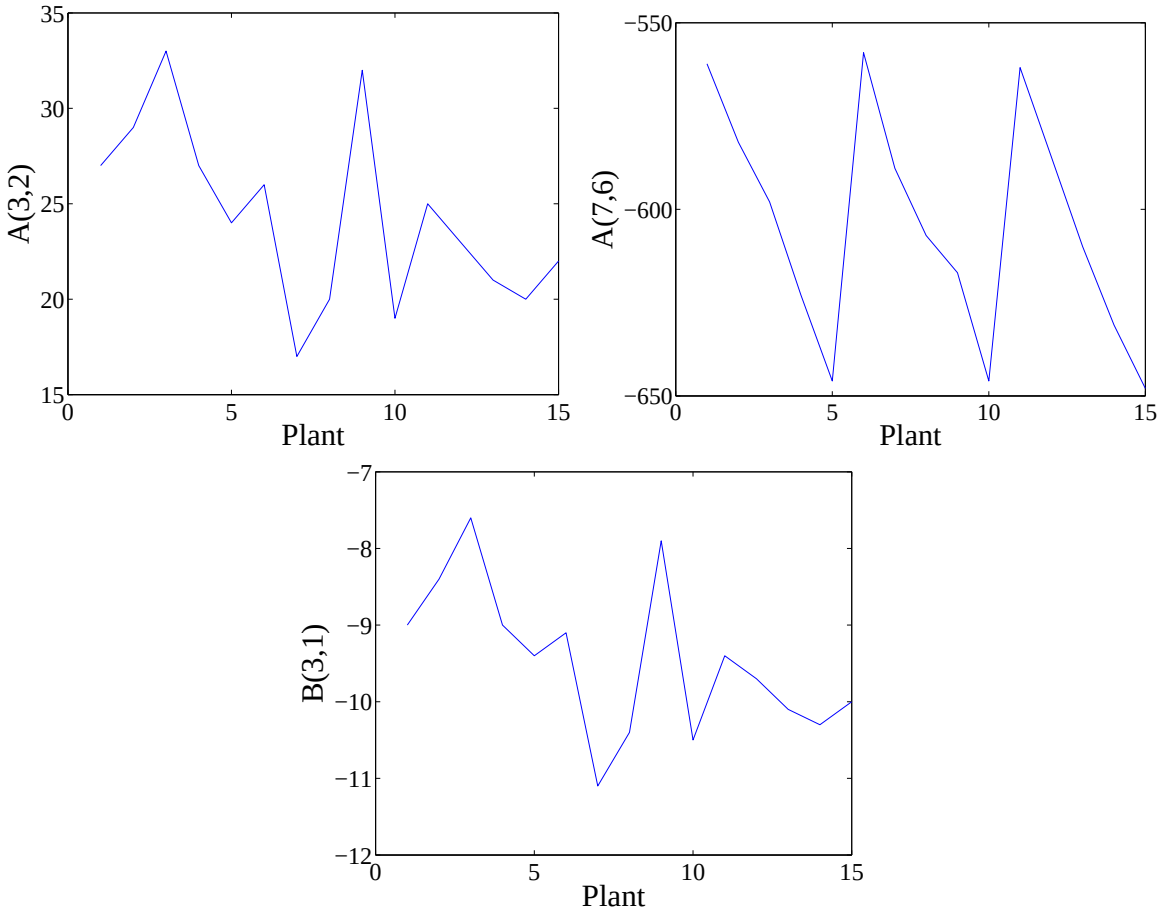

Figure 4-4. Variation in the coefficients of the state matrices

4.2.4 Control Design

To tackle a more rigorous control problem, the dynamics have been augmented to increase the effect of the first flexible mode. It is also observed that the components of states of the second and the third flexible modes do not significantly affect the rigid body dynamics and vice versa. In order to improve the computational efficiency of the simulations, these components have been truncated in this analysis.

A nominal H_∞ controller is created to stabilize the vehicle for all the temperature profiles, so that the structural dynamics controller will not try to alter the rigid-body

dynamics. It also simplifies the process of developing the LPV controller. This nominal controller will be eliminated in future analysis.

To get a quick glimpse of the open-loop system properties like controllability, the temperature profiles are related with the different H_∞ norms for the open-loop stable systems (Figure 4-5). It can be expected that better performance is achieved when the vehicle is cooler and the gradient of the temperature profile does effect the performance. The trend shown by the open-loop norm seems to be similar to the coefficient $A(7,6)$. To explore the relationship between the open-loop norm and $A(7,6)$ a bit more, the norm is plotted as a function of the open-loop dynamic coefficient (Figure 4-6). Such relationships between the performance metric and the open-loop dynamics will be explored more in future analysis.

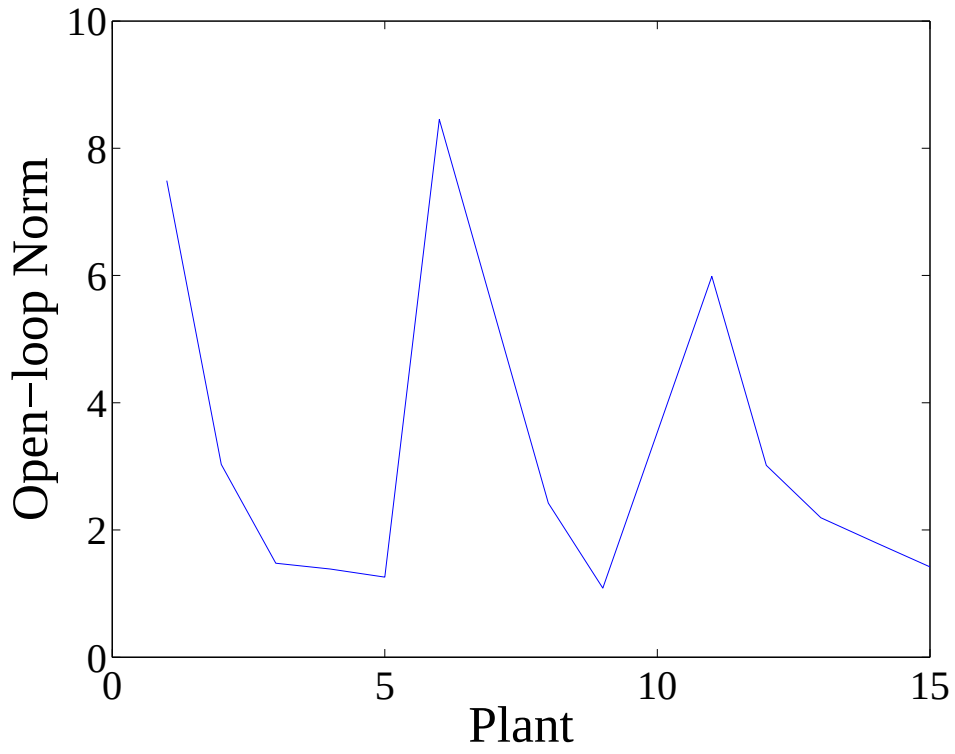

Figure 4-5. H_∞ norm for the different temperature profiles

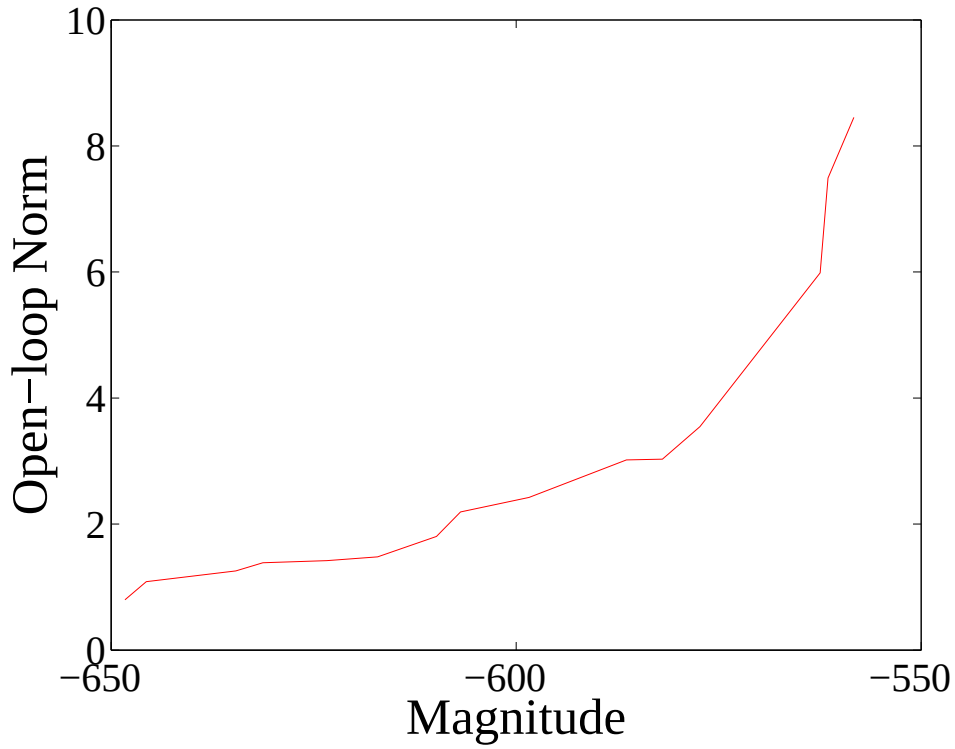

Figure 4-6. Open-Loop norm parameterized around open-loop dynamics

4.2.4.1 Open-loop synthesis

The objective of the LPV controller is to damp out the first flexible mode; i.e. it should reduce the influence of temperature variations on the vehicle without altering the low frequency rigid-body dynamics. The first step in finding the controller is to develop the synthesis model (Figure 4-7).The open-loop system has an unstable rigid-body mode and for most cases is non-minimum phase.

A synthesis model (Figure 4-7) was formulated that relates the open-loop dynamics to a set of errors and disturbances. These errors are specifically chosen such that their size is directly inverse to the closed-loop performance for vibration attenuation.

A model-matching approach is chosen to specify a desired level of vibration attenuation. As such, a target model is given as T in the synthesis model that represents dynamics with appropriate damping on the structural mode. The transfer functions are shown for both the nominal open-loop dynamics and the target dynamics (Figure 4-8).

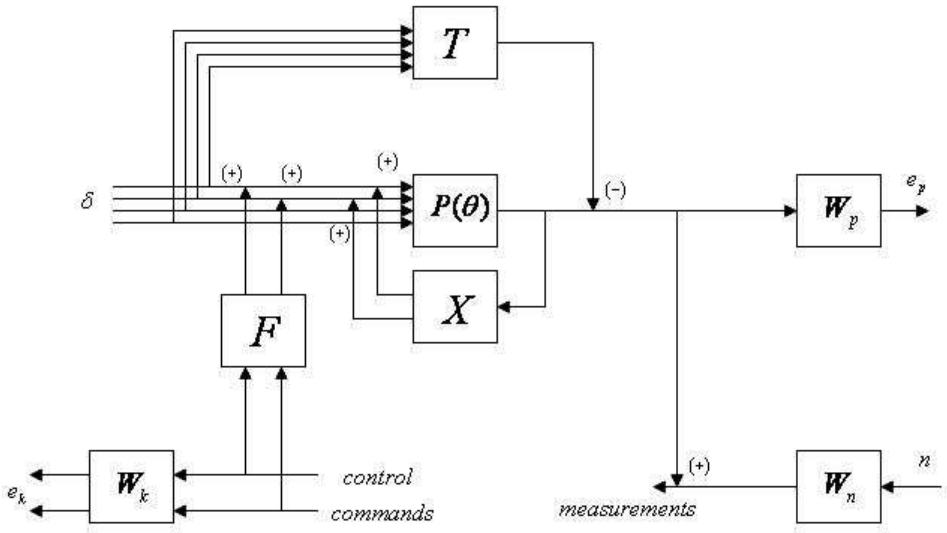

Figure 4-7. Synthesis block diagram

Note the peak near 0.04 *rad/s* is associated with a rigid-body flight mode while the peak near 22 *rad/s* is associated with the structural mode that should be attenuated. So the objective of the inner-loop controller is to get the actual response as close as possible to the target response, especially near the first bending mode without altering the low frequency dynamics.

The system has six input vectors and five output vectors. The input vector, $n \in \mathbb{R}$ is random noise which affects the sensor measurements. The input vector $\delta \in \mathbb{R}^4$ corresponds to the four inputs to the system i.e elevator deflection, canard deflection, diffuser area ratio and the fuel flow ratio. The input vector, $u \in \mathbb{R}^2$ is the control command affecting the actuators. The output vector, $e_p \in \mathbb{R}$ is the weighted measurements of the pitch rate as measured by the sensors. The output vector measurements are the sensor measurements used as feedback to the controller.

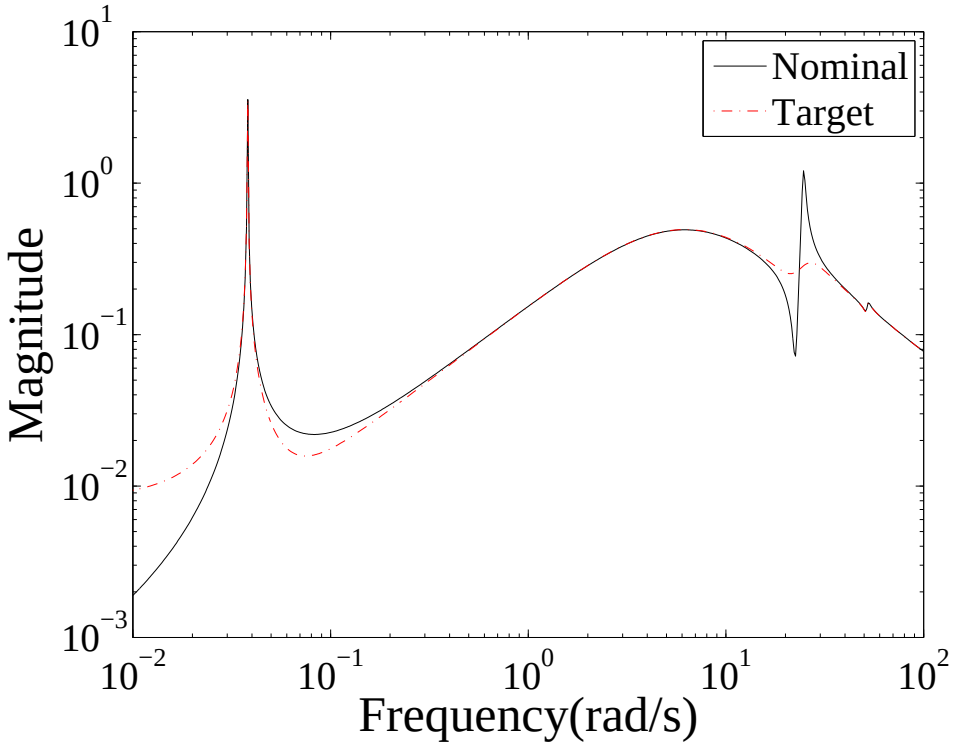

Figure 4-8. Transfer function for the nominal model and target model

A feedback compensator is given as X in the synthesis model. This compensator is only included to stabilize the open-loop dynamics. Essentially, the controller is being designed only to augment damping of the structural mode without introducing any variations to the low-frequency behavior. The $\mathcal{H}_\infty$-norm synthesis is required to stabilize the closed-loop system so X is included to ensure the resulting controller does not affect the rigid-body modes through stabilization. The final multi-loop architecture will introduce an outer-loop controller to replace X and provide both stability and performance for the rigid-body maneuvering.

An error signal, $e_p \in \mathbb{R}$, is defined to represent the tracking performance. This signal is a weighted difference between the actual pitch rate and the desired pitch rate. The weighting, $W_P = \frac{s+100}{s+5}$, is chosen to reflect the frequency range over which tracking is desired.

An error signal, $e_K \in \mathbb{R}^2$, is defined to represent the actuation penalty on elevator and canard. This signal is generated by weighting the command to each surface through $W_k = \frac{s+10}{s+100}$ to reflect a larger penalty on high-frequency actuation. Noise, n, is associated with the sensor measurement of pitch rate. This signal is weighted through $W_n = 0.01$ to limit the relative size of this noise in comparison to the pitch rate. The frequency dependent weighting functions are used to indicate the relative importance of some components of the vector signal and for unit scaling. It is also used for rejecting errors in a certain frequency range. The way the software is written, an input filter, F needs to be introduced into the system. It does not have any physical significance in the system.

Results of the open-loop synthesis is used to create the LPV controller, $K(\theta)$, using the LMI *Control Toolbox* (59). To determine how well the LPV controller will work, H_∞ point controllers are developed for plants corresponding to the different temperature profiles and the results are compared for the two controllers .

4.2.4.2 Closed-loop modeling

Once the LPV controller $K(\theta)$ are formed, controllers for each of the temperature profiles are extracted and connected to make a closed-loop system (Figure 4-9).

The closed-loop system has four inputs and eleven outputs corresponding to the eleven states. K is the controller used to damp out the undesired structural dynamics.

4.2.5 Results

The frequency domain and time domain responses are obtained and compared for the open-loop system, the closed-loop system with the H_∞ controller and the closed-loop system with the LPV controller. The closed loop performance metric, H_∞ norms for the closed-loop synthesis model with the point and the LPV controller are compared (Table 4-2),(Figure 4-10). The small gain theorem needs the closed-loop H_∞ norms of the system be less than or equal to one for control applications to guarantee robust performance with respect to the objective. As the norm from the H_∞ controller is less than one, it ensures better performance than the LPV controller. One of the limitations

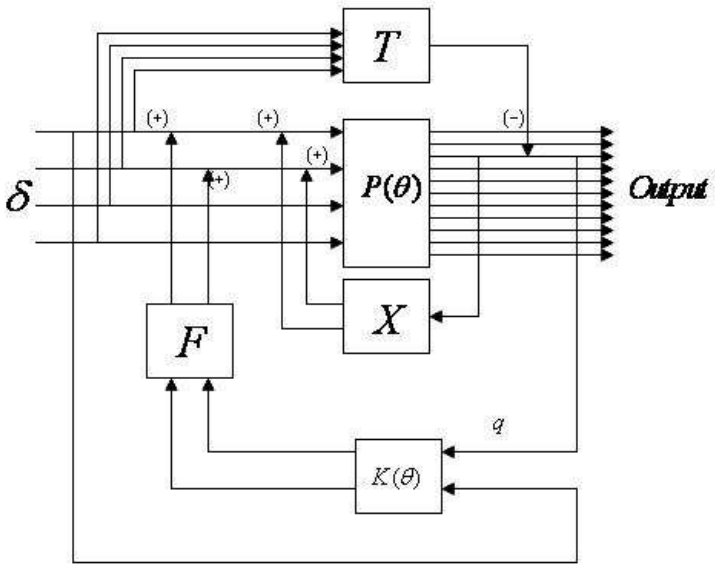

Figure 4-9. Closed-loop design

of the mathematical formulation in the LPV framework is that it assumes that the system can change extremely fast from one temperature profile to another which cannot happen in reality, the variations in heating is a time dependent process. Another limitation of the LPV formulation is that every section of the fuselage can attain any temperature, but it is expected that the temperature decreases from the nose to the tail of the fuselage. Since the trend shown by the open-loop norm is not similar to the trend shown by the closed-loop norm, it can be concluded that the best open-loop system need not necessarily give the best closed-loop performance, at least for this system.

Table 4-2. H_∞ norms for system with H_∞ and LPV controller

Model	H_∞	LPV
1	0.3824	5.0492
2	0.2775	2.5998
3	0.2694	0.8769
4	0.3796	4.9790
5	0.5141	6.8835

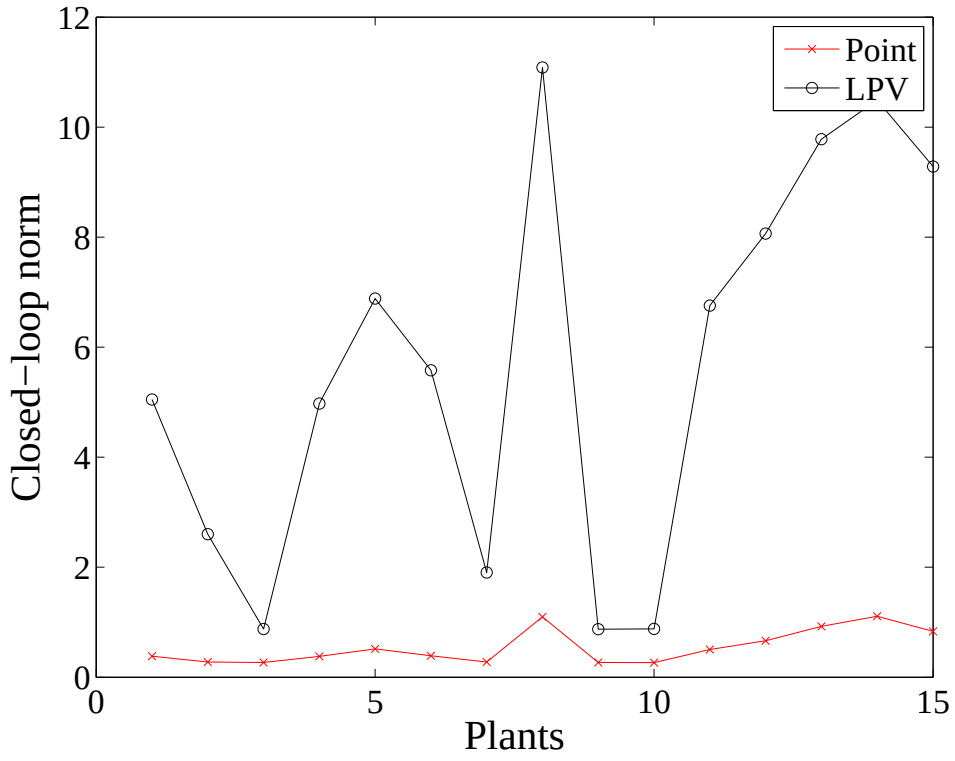

Figure 4-10. Norms of the closed-loop systems

The transfer functions for the open loop system, closed-loop system with the H_∞ controller and with the LPV controller for the five linear temperature profiles are plotted (Figure 4-11). It can be seen that the LPV controller achieves the objective of damping out the first bending mode.

The time response of the open loop, closed-loop systems with the H_∞ controller and with the LPV controller are plotted (Figure 4-12). The open-loop time response shows oscillations which is due to the lack of structural damping and should be eliminated by the controller. It can seen that the LPV and the H_∞ controllers add damping to the system and the oscillations are eliminated.

In order to understand the system a bit better, a pole-zero analysis is performed. The pole-zero map of the closed-loop system with H_∞ and with the LPV controller for the nominal plant model were analyzed (Figure 4-13). The target model has an undershoot in the time response as it is designed on the basis of the open-loop system which is a

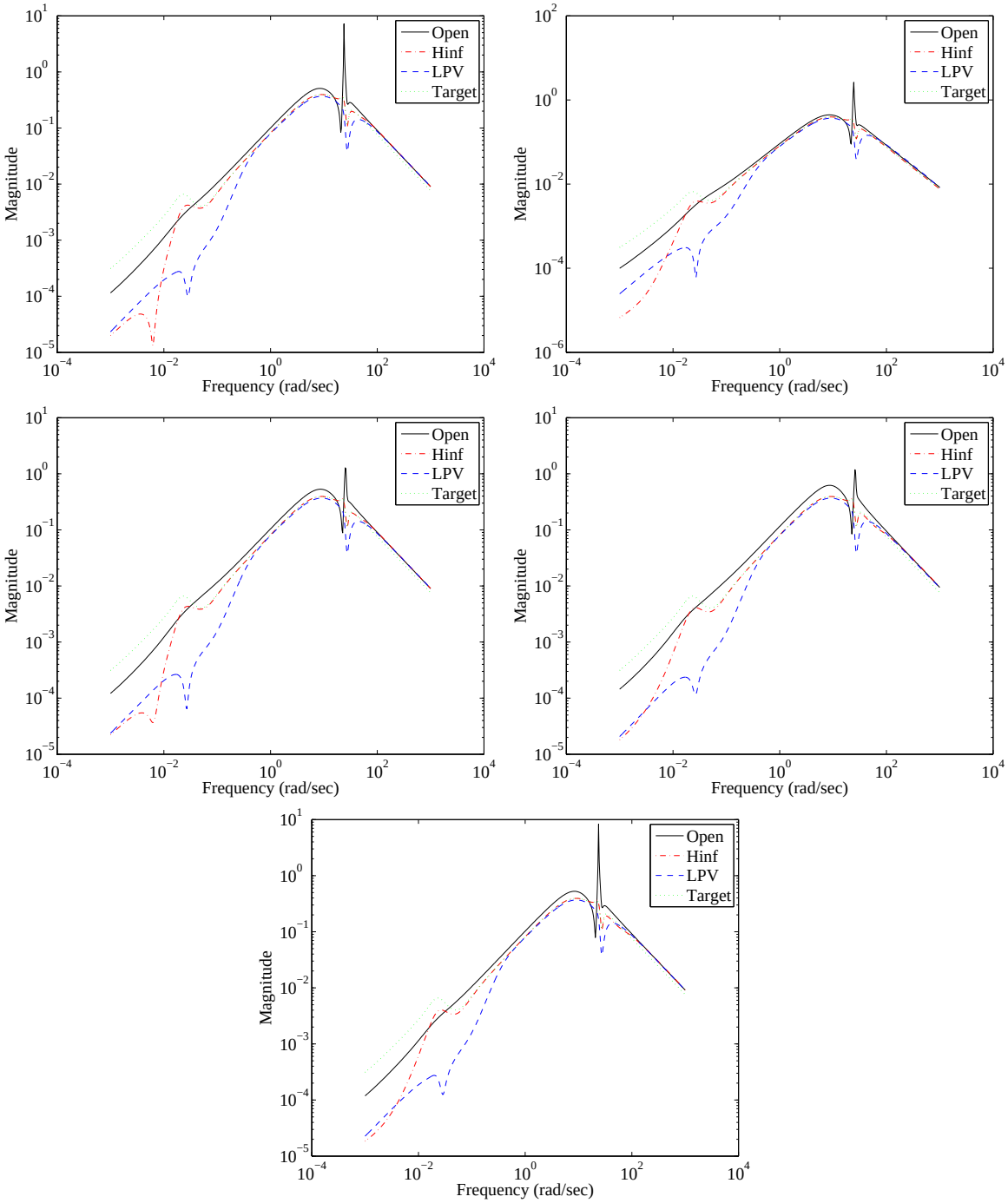

Figure 4-11. Comparison of the transfer functions for the different systems

non-minimum phase and unstable system. Since, this is a 'model-matching' approach an undershoot should be expected in the closed-loop time response. Robust performance for guidance or maneuvering will be guaranteed by the outer-loop controller.

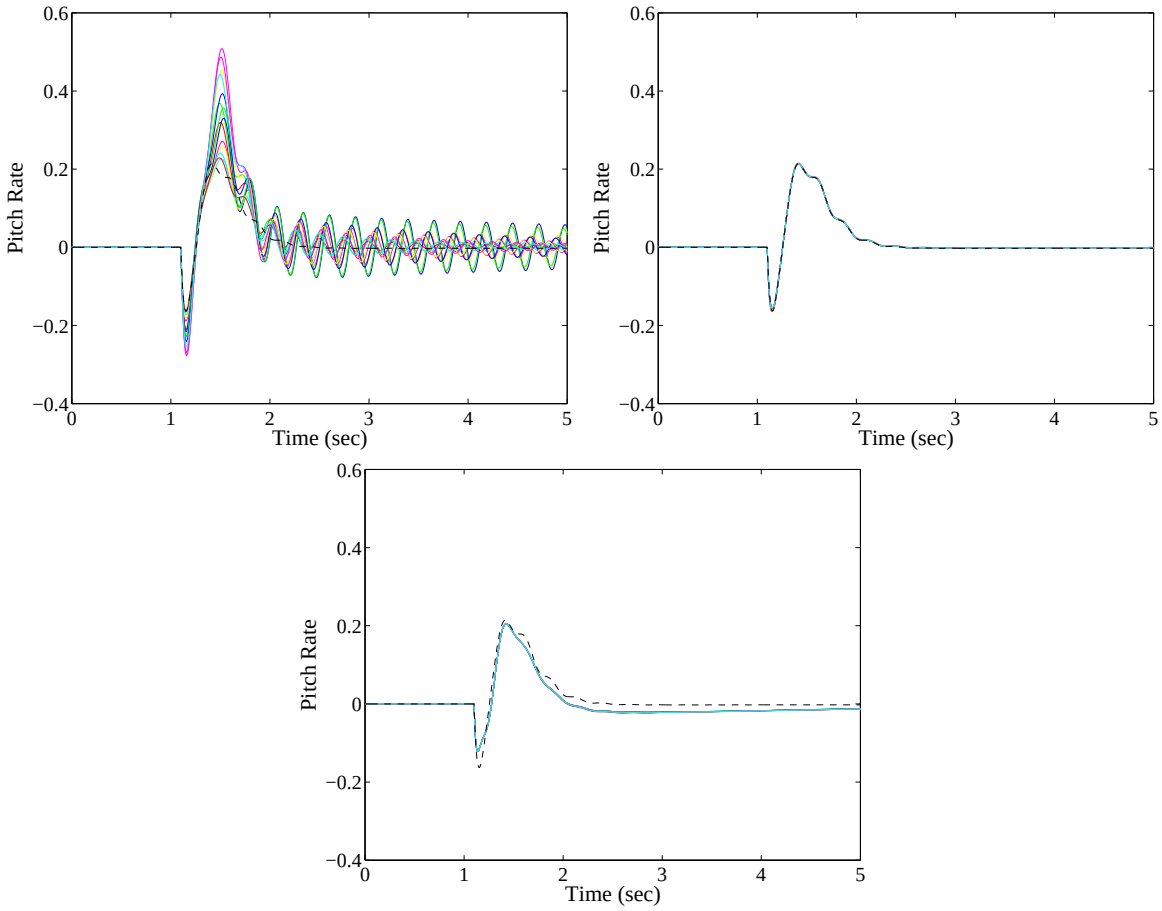

Figure 4-12. Time response for the open-loop and closed-loop systems with the point and LPV controllers

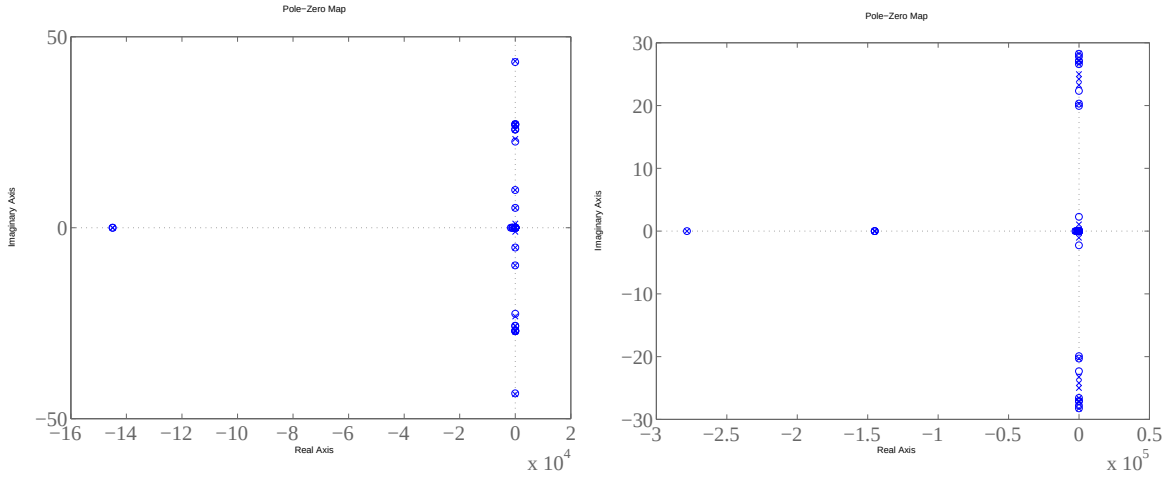

Figure 4-13. Pole-zero map of the closed-loop system with H_∞ and LPV controllers

4.3 Control-Oriented Analysis

The above analysis showed that the approach of having a 'multi-loop' control architecture with the inner-loop LPV controller damping out the undesired dynamics and the outer-loop controller used to achieve robust performance is satisfactory. Using this analysis, important structural information can be sought, i.e. can the vehicle be designed in such a way that it would be easier to control it. The next part of this study tries to address this problem of 'control-oriented design'.

4.3.1 Design Space

In this study, the design space for the open-loop dynamics consists of a 2-dimensional set, $\mathbb{P}$, related to effective temperature. In this case, a set of thermal profiles are chosen that have constant gradient from the nose to tail. This set, (Figure 4-14), considers variations in both the tail temperature and nose temperature (Table 4-3).

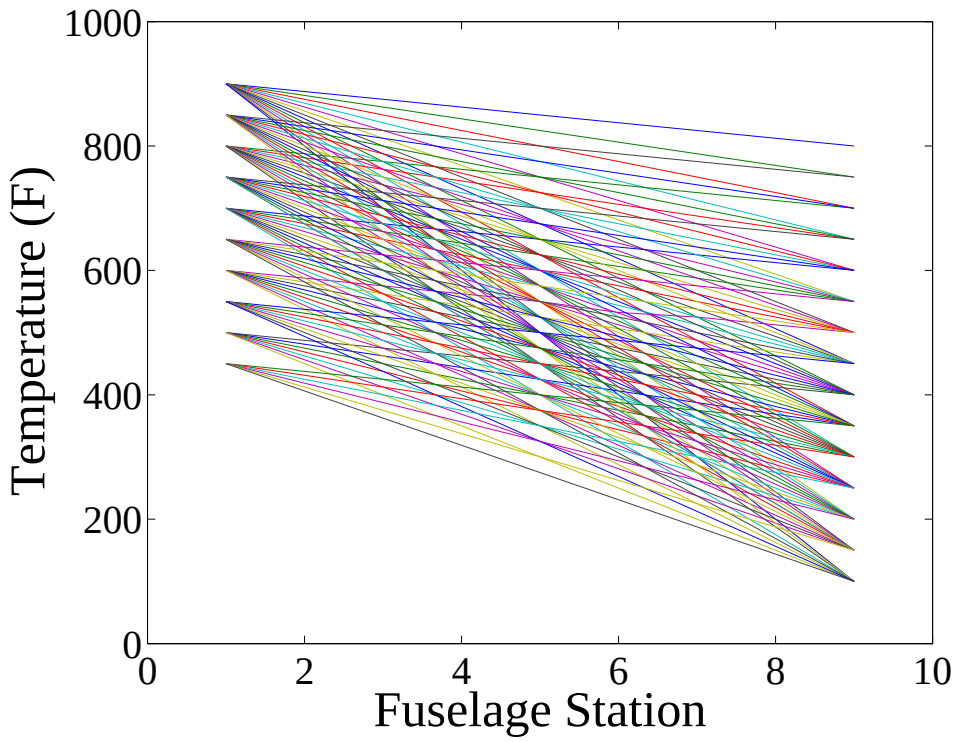

Figure 4-14. Thermal profiles comprising the design space

Table 4-3. Temperature gradients

Set	T_{nose}	Range of T_{tail}
1	900	800-100
2	850	750-100
3	800	700-100
4	750	650-100
5	700	600-100
6	650	550-100
7	600	500-100
8	550	450-100
9	500	400-100
10	450	350-100

The open-loop dynamics are parametrized as a function of these effective temperatures to reflect variations in the Young's modulus at the nose and tail which result from the structural elements and thermal protection system. A set of variables that are representative of the parametrization around the design space are noted, (Figure 4-15) for the influence of bending-mode displacement on the velocity and, (Figure 4-16), for the influence of elevator on the bending-mode velocity.

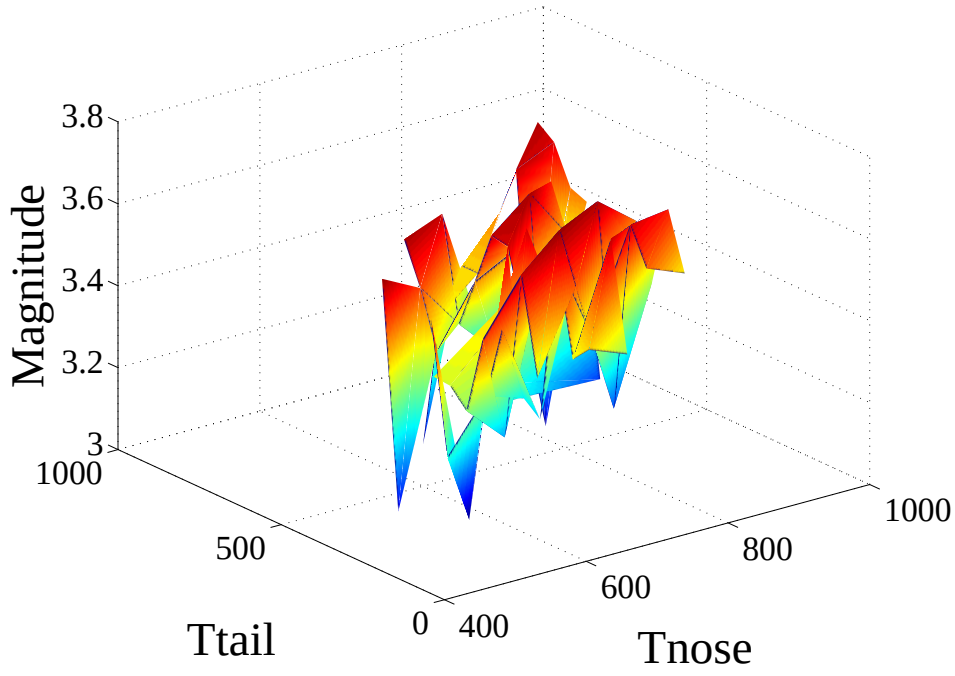

Figure 4-15. Open-loop stability coefficient as a function of the design space

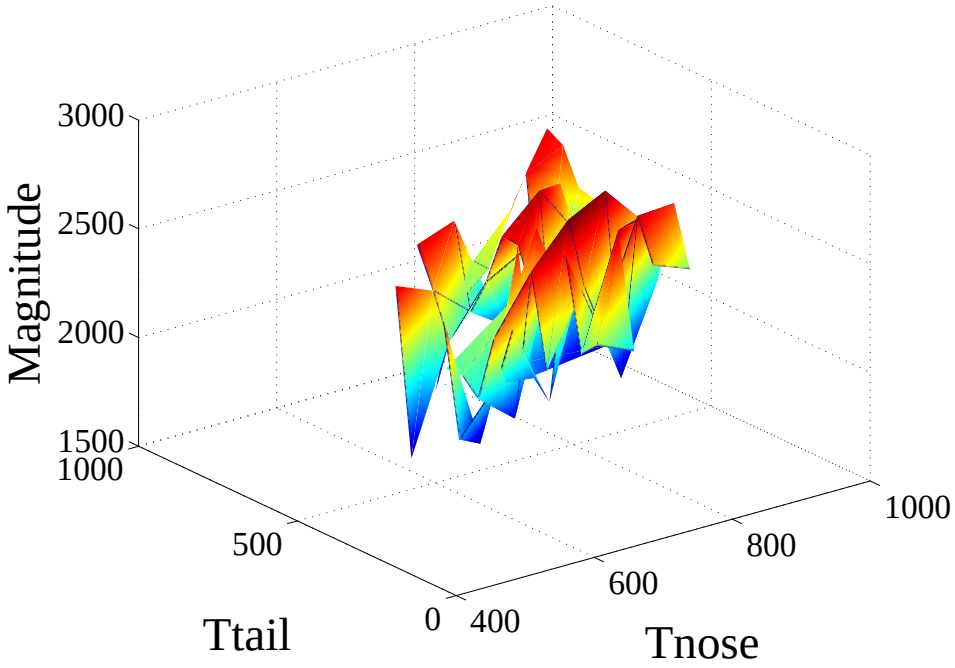

Figure 4-16. Open-loop control coefficient as a function of the design space

The design space is limited to $\mathbb{P}$ which contains parameters for the fuselage structure and the thermal protection system along with $\mathbb{K}$ which contains parameters for a feedback controller. Such limitations note that the geometry is relatively fixed due to aerodynamic issues while the thermal issues and structural dynamics have considerable freedom in their design. In this case, the design space is appropriate since the thermal protection system and structure interact to determine the vibration characteristics of the fuselage along with associated heating effects.

4.3.2 Control-Oriented Design

A control-oriented design is optimized for a hypersonic vehicle. The design is performed to choose the structure and thermal protection system along with the controller. In this case, an $\mathcal{H}_\infty$-norm synthesis is used that considers the pair of parametrized Riccati equations. A basic algorithm for constrained optimization generates a design that corresponds to a local minimum of the cost function.

The optimal elements of the design space are chosen as $\pi = [750, 450]$ and the controller, κ, whose Bode plot is shown, (Figure 4-17). As such, the value of π indicates the lowest closed-loop norm is achieved if the thermal protection system is chosen to have a nose temperature of 750^oF and a tail temperature of 450^oF.

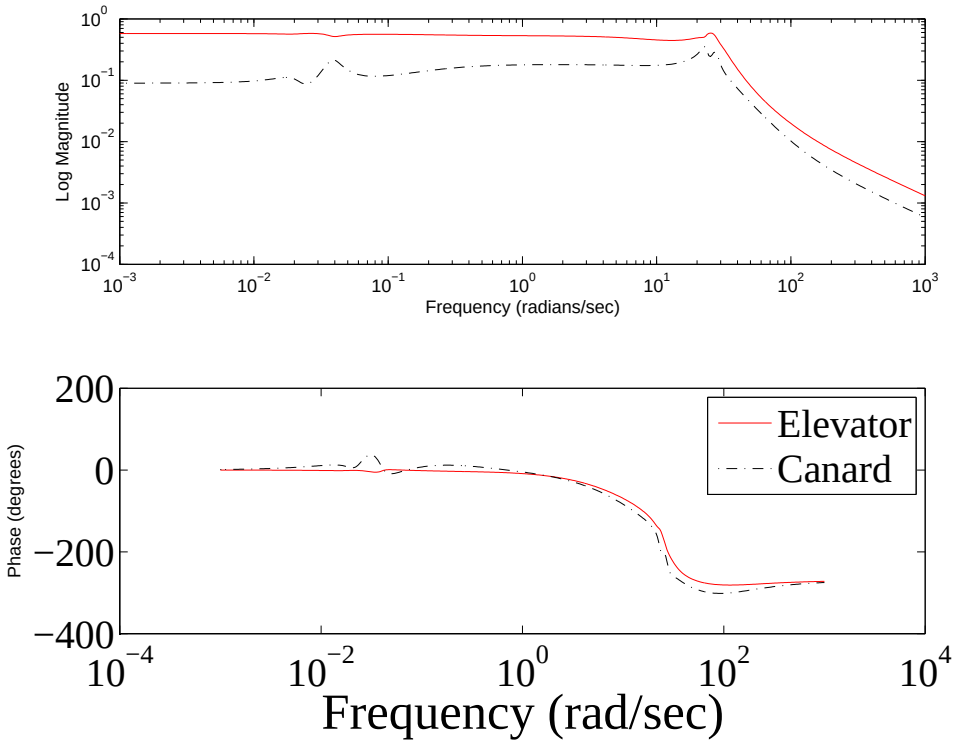

Figure 4-17. Optimal controller from pitch rate to elevator and canard deflection

The transfer function of the closed-loop system (Figure 4-18) is similar to the transfer function of the target model. The relationship between pitch rate and elevator are close at all frequencies but particularly close near the natural frequency of the bending mode. As such, the objective of high-frequency vibration attenuation without altering the low-frequency dynamics is essentially achieved. The time response of the input elevator deflection for the profile giving optimal performance (Figure 4-19) and the resulting vibration attenuation and associated actuation are plotted (Figure 4-20).

The optimality of the system can be verified by comparing the performance metrics for the control-oriented design to a complete design over system in the design space. This

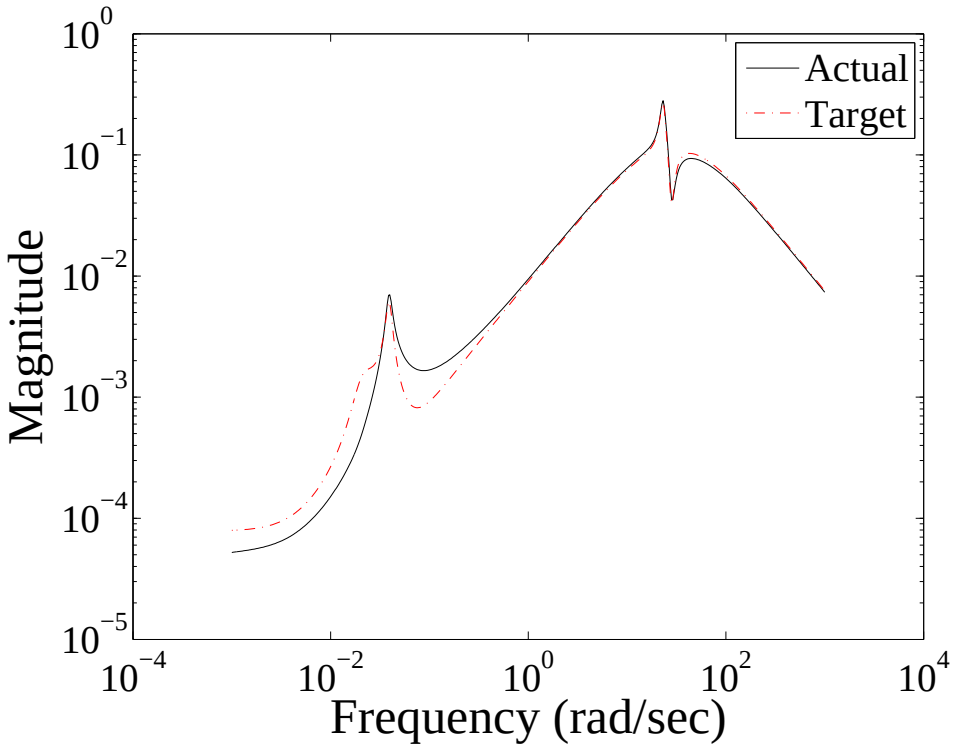

Figure 4-18. Actual and desired transfer function

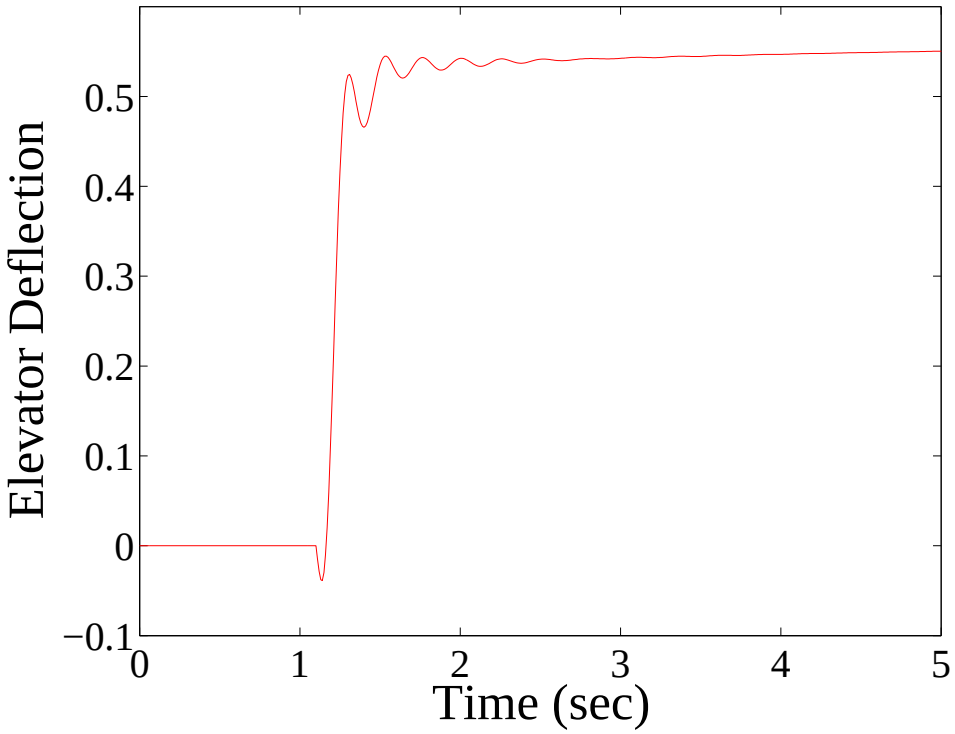

Figure 4-19. Input elevator deflection

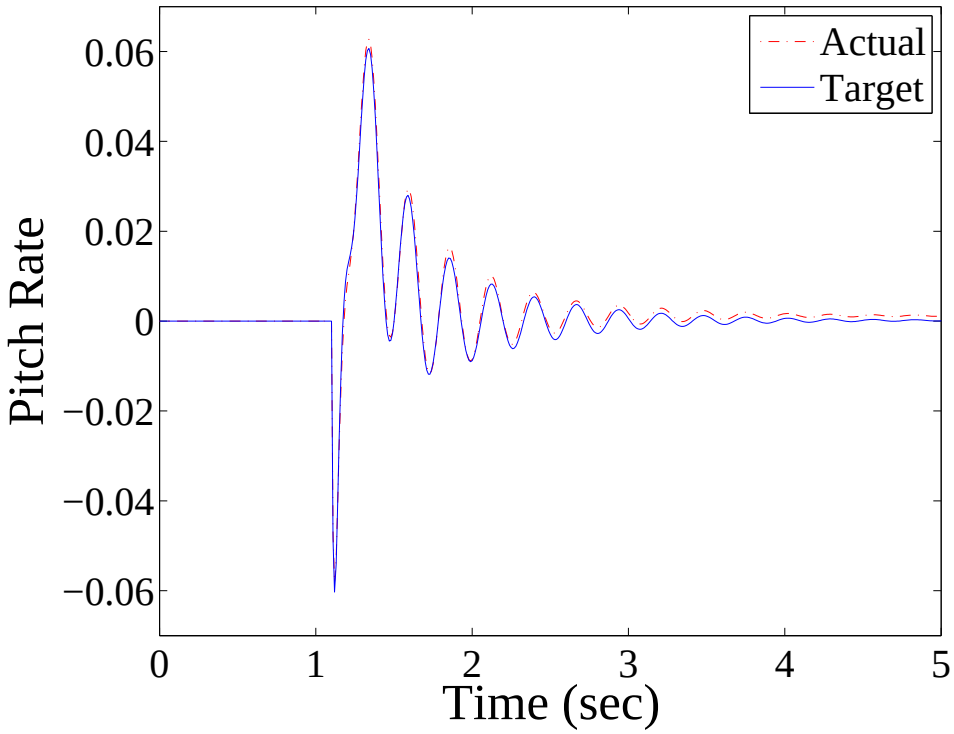

Figure 4-20. Actual and desired closed-loop response

comparison is relatively easy to do for this system; however, it would be prohibitive to compute closed-loop designs for each configuration with a high-dimensional design space. In this case, the control-oriented design is able to achieve a closed-loop norm of 0.22.

4.3.3 Analysis

The relationship between the design space and the closed-loop performance can be explored. In particular, the complexity between open-loop design and closed-loop design should be evaluated to determine the additional cost induced by the addition of control synthesis to the procedure.

The difficulty of optimizing an open-loop design are understood. Certainly the open-loop dynamics, (Figure 4-15), have a highly nonlinear parameterization around the design space. A functional based on this nonlinear parametrization would thus have to be minimized to obtain optimality in any open-loop design.

The closed-loop norm can similarly be parametrized around the design space. In this case, a set of controllers are generated for each thermal profile (Figure 4-14) and

associated open-loop plant (Figure 4-15). The resulting closed-loop norm, (Figure 4-21), shows a remarkably similar parametrization as the open-loop dynamics.

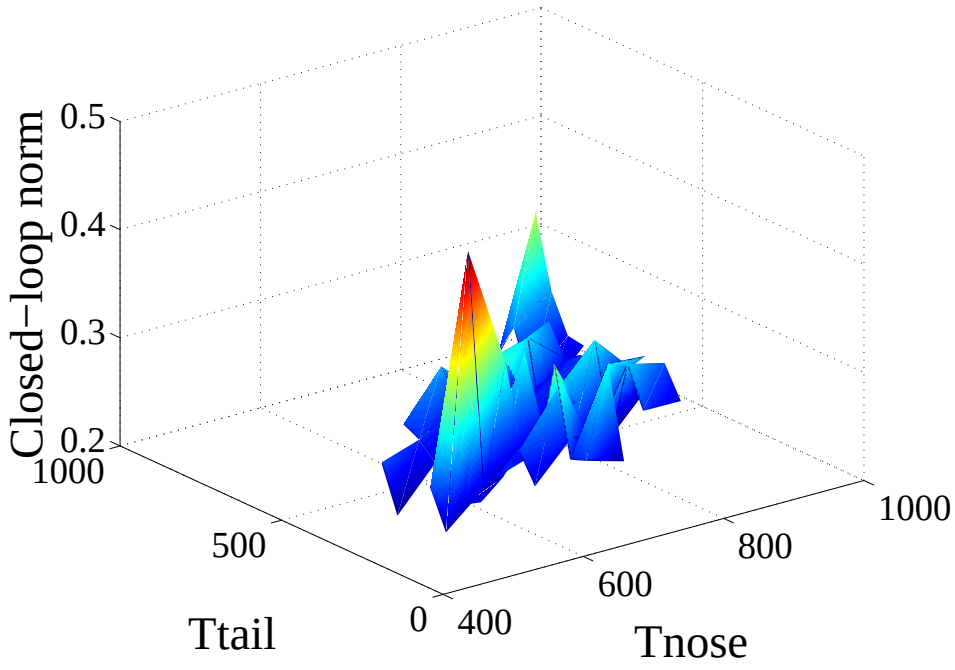

Figure 4-21. Closed-loop norm parametrized around the design space

It was noticed that quiet a few coefficients of the A and B matrix of the open-loop dynamics vary with temperature. On further investigation, it can be noted that the coefficients which vary with temperature can be put into two groups. The first group consists of coefficients which show the same trend as in the closed-loop norm and the second group consists of coefficients which show the opposite trend to the closed loop-norm (Table 4-4).

The reason for the similarity between parameterizations of open-loop dynamics and closed-loop dynamics is found by investigating a different relationship; namely, the closed-loop norm should be parameterized as a function of the open-loop dynamics instead of the design space. The closed-loop norm and associated performance for tracking is actually directly related to the parameters of the open-loop state-space model. This result

Table 4-4. Coefficients of the open-loop dynamics which vary with temperature

Group I	Group II
A(1,6)	A(3,2)
A(3,6)	A(7,4)
A(7,1)	B(1,1)
B(1,3)	B(1,2)
B(7,1)	B(1,4)
A(7,3)	B(3,1)
	B(3,2)
	B(3,3)
	B(3,4)
	B(7,2)
	B(7,2)

is certainly expected; however, the independence of that relationship from temperature (Figure 4-22) is not completely anticipated.

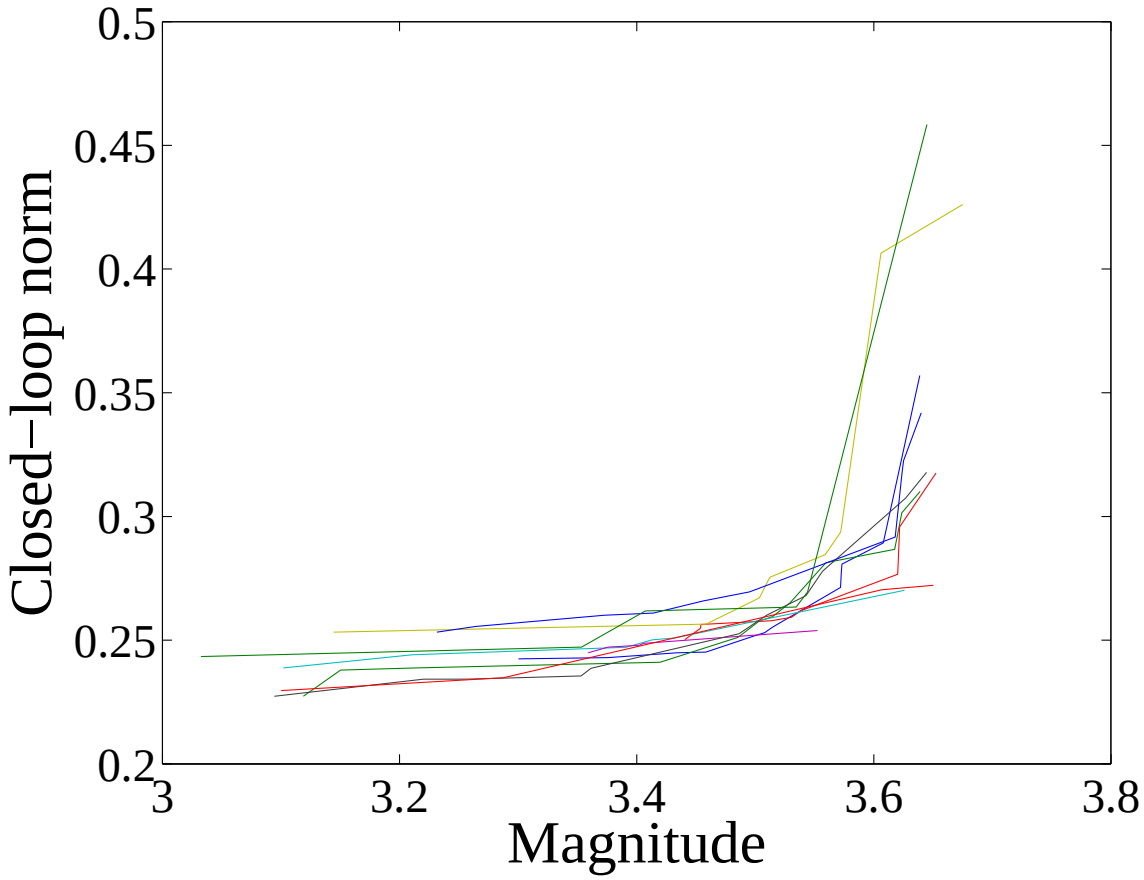

Figure 4-22. Closed-loop norm parametrized around open-loop dynamics

A control-oriented design is thus demonstrated to be similar in difficulty to open-loop design. The introduction of control synthesis merely adds a linear dependency onto a nonlinear dependency which does not overly increase the computational challenge.

4.3.4 Sensitivity

Sensitivity analysis investigate the robustness of mathematical models to variations in the parameters. The sensitivity of the design to nonlinear dependencies should be noted. The dynamics, (Figure 4-15), are strongly nonlinear across the design space so the optimization is almost certain to reach only a local minimum. Such local minima are not necessarily accompanied by poor performance since several such local minima have closed-loop norms within 5% of the global minimum. The data (Figure 4-23) shows that several thermal profiles associated with local minima and the resulting performance (Figure 4-24) can compare favorably with the global minima and its resulting performance.

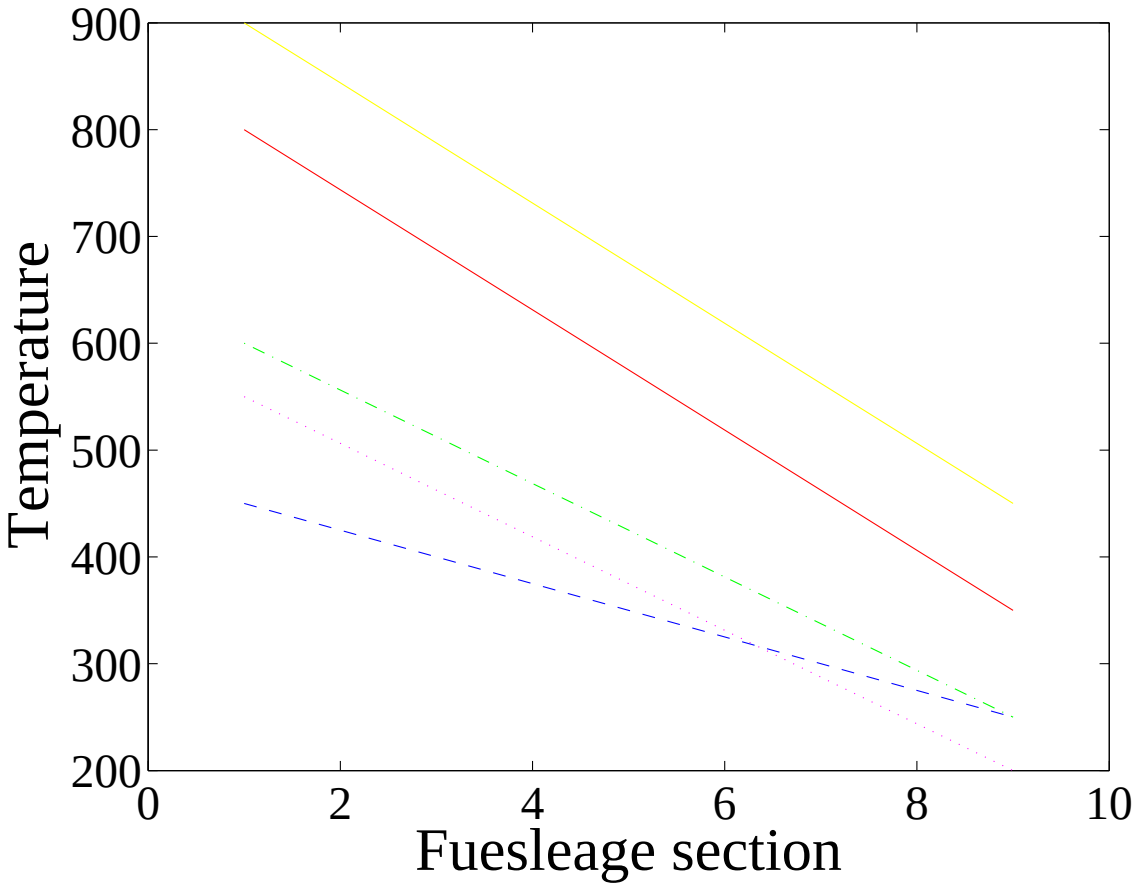

Figure 4-23. Thermal profiles associated with similarly-valued local minima

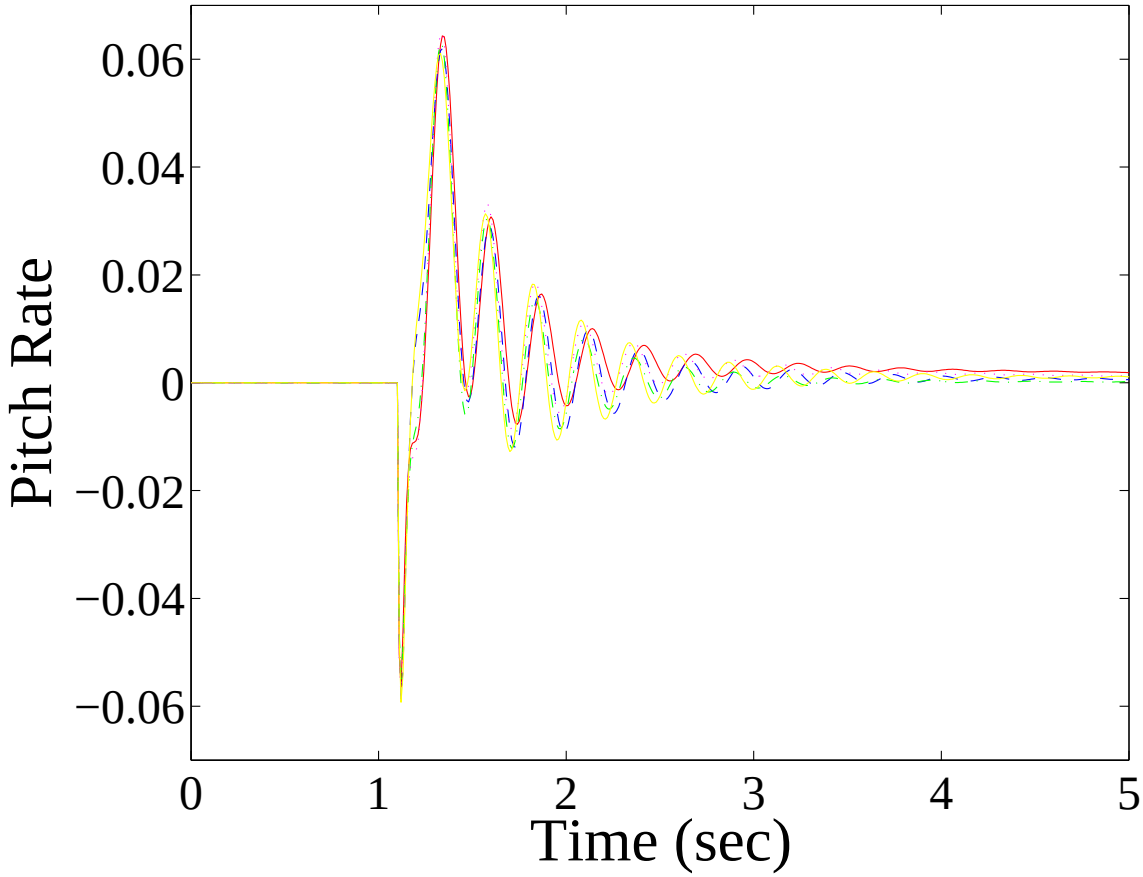

Figure 4-24. Closed-loop performance for each thermal profile

This sensitivity presents an interesting feature of the hypersonic vehicle; namely, similar levels of closed-loop performance can be achieved for several choices of thermal profiles if they are designed properly. The profiles (Figure 4-23) allow for similar closed-loop performance so the associated thermal protection systems can be further evaluated for issues such as weight and cost to optimize the design for additional metrics.

CHAPTER 5
CONCLUSION

Vibration attenuation is a critical requirement for maintaining hypersonic flight for a coupled fuselage-engine configuration. Such attenuation can be facilitated by designing both a thermal protection system (TPS) and a feedback controller that can compensate for the variations in the structural dynamics due to different temperature profiles which vary in time during a hypersonic flight. The first part of this study considered the control of the structural dynamics of an air-breathing hypersonic vehicle using a Linear Parameter Varying (LPV) controller. The effect of temperature variations on the open-loop dynamics of the system was analyzed. Then a Linear Parameter Varying controller is formulated to damp out the undesired dynamics. This type of controller is chosen because the change in the dynamics can be modeled as an affine function of temperature. This controller is then compared with the point controllers at various temperature profiles. The closed-loop H_∞ norms showed that the point controller guarantees performance and the LPV controller does not guarantee performance for all trajectories. However, keeping in mind the mathematical restrictions imposed by the way the Linear Parameter Varying system is formulated, the simulation results show that the LPV controller performs satisfactorily. Hence, the approach of having an inner-loop LPV controller to damp the undesired structural dynamics seems to be a feasible solution. In the second part of this study, a control-oriented design is introduced by which the open-loop system is designed to achieve the maximum level of performance for which a controller exists. A representative model of a hypersonic vehicle is used to demonstrate this approach can indeed generate a design. It is also shown that there are several temperature profiles which give similar level of closed-loop optimal performance.

REFERENCES

[1] Bolender, M., and Doman, D., "A Non-linear Model for the Longitudinal Dynamics of a Hypersonic Air-Breathing Vehicle," AIAA *Guidance,Navigation and Control Conference and Exhibit*, August 2005, AIAA-2005-6255.

[2] Chavez,F., and Schmidt,D.,"Analytical Aeropropulsive/Aeroelastic Hypersonic-Vehicle Model with Dynamic Analysis," *Journal of Guidance,Control and Dynamics*, Vol. 17, No. 6, Nov-Dec 1994, pp. 1308-1319.

[3] Bolender, M., and Doman, D., "Nonlinear Longitudinal Dynamical Model of an Air-Breathing Hypersonic Vehicle," *Journal of Spacecraft and Rockets*, Vol. 44, No. 2, March-April 2007, pp. 374-387.

[4] Bolender,M., and Doman,D., "Modeling Unsteady Heating Effects on the Structural Dynamics of a Hypersonic Vehicle," AIAA *Atmospheric Flight Mechanics Conference and Exhibit*, August 2006, AIAA-2006-6646.

[5] Williams, T., Bolender, M., Doman, D., and Morataya, O., "An Aerothermal Flexible Model Analysis of a Hypersonic Vehicle," AIAA *Atmospheric Flight Mechanics Conference and Exhibit*, August 2006, AIAA-2006-6647.

[6] Culler,A. ,Williams, T., and Bolender, M., "Aerothermal Modeling and Dynamic Analysis of a Hypersonic Vehicle," AIAA *Atmospheric Flight Mechanics Conference and Exhibit*, August 2007, AIAA-2007-6395.

[7] Oppenheimer, M.,Skijins, T.,Bolender, M., and Doman, D., "A Flexible Hypersonic Vehicle Model Developed With Piston Theory," AIAA *Atmospheric Flight Mechanics Conference and Exhibit*, August 2007, AIAA-2007-6396

[8] Buschek,H., and Calise,A., "Fixed Order Robust Control Design for Hypersonic Vehicles," *AIAA Guidance, Navigation and Control Conference*, AIAA-94-3662,1994.

[9] Buschek,H., and Calise,A., "Robust Control of Hypersonic Vehicles Considering Propulsive and Aeroelastic Effects," AIAA *Guidance,Navigation and Control Conference*, 1993, AIAA-93-3762.

[10] Lind,R.,"Linear Parameter-Varying Modeling and Control of Structural Dynamics with Aeroelastic Effects,"*Journal of Guidance,Control and Dynamics*, Vol. 25, No. 4,2001, pp. 733-739.

[11] Jankovsky,P., Sigthorsson,D., Serrani,A. ,Yurkovich,S., Bolender,M., and Doman,D., "Output Feedback Control and Sensor Placement for a Hypersonic Vehicle Model," AIAA *Guidance,Navigation, and Control Conference and Exhibit*, August 2007, AIAA-2007-6327.

[12] Baruth, H., and Choe, K., "Sensor Placement in Structural Control" *Journal of Guidance, Control, and Dynamics*, Vol. 13, No. 3, 1990, pp. 524533.

[13] Xu, K., Warnitchai,P., and Igusa,T., "Optimal Placement and Gains of Sensors and Actuators for Feedback Control," *Journal of Guidance, Control, and Dynamics*, Vol. 17, No. 5, 1994, pp. 929934.

[14] Lim, K., "Method for Optimal Actuator and Sensor Placement for Large Flexible Structures," *Journal of Guidance, Control, and Dynamics*, Vol. 15, No. 1, 1992, pp. 4957.

[15] Tongco, E., and Meldrum, D., "Optimal Sensor Placement of Large Flexible Space Structures," *Journal of Guidance, Control, and Dynamics*, Vol. 19, No. 4, 1996, pp. 961963.

[16] Mirmirani,M., Wu,C., Clark,A., Choi,S., and Colgren,R., "Modeling for Control of a Generic Air breathing Hypersonic Vehicle," *AIAA Guidance, Navigation and Control Conference*, AIAA-2005-6256.

[17] Fiorentini,L., Serrani,A., Bolender,M., and Doman,D., "Nonlinear Robust/Adaptive Controller Design for an Air-breathing Hypersonic Vehicle Model," *AIAA Guidance, Navigation and Control Conference and Exhibit*, August 2007, AIAA-2007-6329.

[18] Sigthorsson,O.,D, Jankovsky,P., Serrani,A., Yurkovich,S., Bolender,A.,M., and Doman,D., "Robust Linear Output Feedback Control of an Air breathing Hypersonic Vehicle," , *Journal of Guidance,Control and Dynamics*, Vol. 31, No. 4, July-August 2008, pp. 1052-1066.

[19] Kuipers, M., Mirmirani, M., Ioannou,P., and Huo, Y., "Adaptive Control of an Aeroelastic Air breathing Hypersonic Cruise Vehicle," August 2007,AIAA Paper 2007-6326.

[20] Sigthorsson,D.,O., Serrani,A., Yurkovich,S., Bolender,M.,A., and Doman,D.,B., "Tracking Control for an Overactuated Hypersonic Air breathing Vehicle with Steady State Constraints," August 2006,AIAA Paper 2006-6558.

[21] Huo,Y., Mirmirani,M., Ioannou,P., and Kuipers,M., "Altitude and Velocity Tracking Control for an Air breathing Hypersonic Cruise Vehicle," August 2006,*AIAA Paper* 2006-6695.

[22] Groves, K.,P., Sigthorsson, D.,O., Serrani,A., Yurkovich,S., Bolender, M.,A., and Doman, D.,B., "Reference Command Tracking for a Linearized Model of an Air breathing Hypersonic Vehicle," August 2005, AIAA Paper 2005-6144.

[23] Groves, K.,P., Serrani,A., Yurkovich,S., Bolender,M.,A., and Doman, D.,B., " Anti-Windup Control for an Air breathing Hypersonic Vehicle Model," August 2006, AIAA Paper 2006-6557, .

[24] Parker,T.,J., Serrani,A., Yurkovich,S., Bolender,A.,M., and Doman,B.,D., "Control-Oriented Modeling of an Air-Breathing Hypersonic Vehicle," *Journal of Guidance,Control, and Dynamics*, Vol. 30,No. 3,2007,pp. 856-869.

[25] Safonov,G.,M., Goh,C.,K., and Ly,H.,J., "Control System Synthesis via Bilinear Matrix Inequalities," *IEEE American Control Conference*, 1994, pp. 45-49.

[26] Shi,G., and Skelton,E.,R., "An Algorithm for Integrated Structure and Control Design with Variance Bounds," *IEEE Conference on Decision and Control*, 1996, pp. 167-172.

[27] Tanaka,T., and Sugie,T., "General Framework and BMI Formulae for Simultaneous Design of Structure and Control Systems," *IEEE Conference on Decision and Control*, 1997, pp. 773-778.

[28] Tuan,D.,H., and Apkarian,P., "Low Nonconvexity-Rank Bilinear Matrix Inequalities: Algorithms and Applications in Robust Controller and Structure Design," *IEEE Transactions on Automatic Control*, Vol. 45, No. 11, November 2000, pp. 2111-2117.

[29] McNamara,J.,J., and Friedmann,P.,P., "Aeroelastic and Aerothermoelastic Analysis of Hypersonic Vehicles: Current Status and Future Trends," AIAA *Structures, Structural Dynamics, and Materials Conference*, April 2007, AIAA-2007-2013.

[30] McNamara,J., Friedmann,P., Powell,K., and Thuruthimattam,B., "Aeroelastic and Aerothermoelastic Vehicle Behavior in Hypersonic Flow," AIAA/CIRCA *13th International Space Planes and Hypersonic Systems and Technologies*, 2005,AIAA-2005-3305.

[31] Bisplinghoff, R.L. and Dugundji, J., "Influence of Aerodynamic Heating on Aeroelastic Phenomena in High Temperature Effects in Aircraft Structures," *Agardograph* No. 28, Edited by N.J. Hoff, Pergamon Press, 1958, pp. 288-312.

[32] Garrick, I.E., "A Survey of Aerothermoelasticity," *Aerospace Engineering*, January, 1963, pp. 140-147.

[33] Ricketts, R., Noll, T., Whitlow, W., and Huttsell,L., "An Overview of Aeroelasticity Studies for the National Aerospace Plane," Proc. 34th AIAA/ASME/ASCE/AHS/ASC Structures, Structural Dynamics and Materials Conference, April 1993, pp. 152-162.

[34] Thuruthimattam, B.,J., Friedmann, P.,P., McNamara, J.,J., and Powell, K.,G., "Aeroelasticity of a Generic Hypersonic Vehicle," *Proc. 43rd AIAA/ASME/ASCE/AHS Structures, Structural Dynamics and Materials Conference*, April 2002,AIAA Paper No. 2002-1209.

[35] Thuruthimattam, B.,J., Friedmann, P.,P., McNamara, J.,J., and Powell, K.,G., "Modeling Approaches to Hypersonic Aerothermoelasticity with Application to Reusable Launch Vehicles," *Proc. 44th AIAA/ASME/ASCE/AHS Structures, Structural Dynamics and Materials Conference*, April 2003, AIAA Paper No. 2003-1967.

[36] Rogers, M., "Aerothermoelasticity," *AeroSpace Engineering*, October 1958, pp. 34-43.

[37] Bisplinghoff, R.,L., Ashley, H., and Halfman, R.,L., *Aeroelasticity*, Addison-Wesley, 1955.

[38] Lind,R., Buffington,J., and Sparks,A., "Multi-Loop Aeroservoelastic Control of a Hypersonic Vehicle," AIAA Paper 99-4123.

[39] Vosteen, L.,F., "Effect of Temperature on Dynamic Modulus of Elasticity of Some Structural Alloys," NACA, TN 4348, August 1958.

[40] Waszak, M.,R., Buttrill, C.,S., and Schmidt, D.,K., "Modeling and Model Simplification of Aeroelastic Vehicles: An Overview," NASA TM-107691, 1992.

[41] Meirovitch,L., and Tuzcu,I., "Integrated Approach to the Dynamics and Control of Maneuvering Flexible Aircraft," NASA CR-2003-211748, 2003.

[42] McLean,D., "Automatic Flight Control Systems", Prentice-Hall International, Hertfordshire, UK, 1990.

[43] Theodore,R.,C., Ivler,M.,C., Tischler,M.,B., Field,J.,E., Neville,L.,R., and Ross,P.,H., "System Identification of Large Flexible Transport Aircraft," *AIAA Atmospheric Flight Mechanics Conference and Exhibit*, 2008, AIAA-2008-6894.

[44] Heeg,J., Zeiler,A.,T., Pototzky,S.,A, Spain,V.,C., and Engelund,C.,W., " Aerothermoelastic Analysis of a NASP Demonstrator Model," *AIAA Structures, Structural Dynamics, and Materials Conference*, 1993, AIAA-93-1366-CP.

[45] Leith,D., and Leithead,W.,"Survey of Gain-Scheduling Analysis & Design," International Journal of Control,73: 11,2000,pp.1011- 1025.

[46] Fitzpatrick,K.,"Control of the Structural Dynamics of a Hypersonic Vehicle Across a Temperature Range," AIAA-RISC-2003-U-002.

[47] Mazzaro,C.,M., Movsichoff,A.,B., Pena,S.,S.R., "Robust Identification of Linear Parameter Varying systems," *American Control Conference*,1999,pp. 2282-2284.

[48] Bamieh,B., Giarre,L., "Identification of Linear Parameter Varying Models," *IEEE Conference on Decision and Control*,1999,pp. 1505-1510.

[49] Verdult,V.,and Verhaegen,M.,"Identification of Multi variable LPV State Space Systems By Local Gradient Search," *European Control Conference*, 2001, pp. 3675-3680.

[50] Nakajima,A., and Tsumura,K.," Identification of LPV MIMO Systems," *SICE Annual Conference*, Vol. 2, 2002, pp. 1241-1245.

[51] Verhaegen,M., and Dewilde,P., "Subspace Model Identification Part I: The Ouput error State Space Model Identification Class of Algorithms," *International Journal of Control*, Vol. 56,1992, pp. 1187-1210.

[52] Kumar,A., and Anderson,M., "A Comparison of LPV Modeling Techniques for Aircraft Control," *AIAA Guidance Navigation and Control Conference*, AIAA-2000-4458,2000.

[53] Azuma,T., Watanabe, R., and Uchida, K.,"An Approach to Solving Parameter-Dependent LMI Conditions Based on Finite Number of LMI Conditions," *IEEE American Control Conference* ,1991, pp. 510-514.

[54] Shamma,S.J., Cloutier,R.,J., "Gain Scheduled missile Autopilot Design Using Linear Parameter Varying Transformations," *Journal of Guidance,Control and Dynamics*, Vol. 1, No. 2, 1993, pp. 69-79.

[55] Wu,F., and Packard,A.,"LQG Control Design for LPV Systems," *American Control Conference*, Vol. 6, June 1995, pp. 4440-4444.

[56] Apkarian,P., Gahinet,P., and Becker,G., " Self-Scheduled H_∞ Control of Linear Parameter Varying Systems," *IEEE Conference on Decision and Control*, Vol. 3, 1994, pp. 2026-2031.

[57] Apkarian,P., and Gahinet,P., "A Convex Characterization of Gain-Scheduled H_∞ Controllers," *IEEE Transactions on Automatic Control*, Vol. 40, No. 5,1995, pp. 853-864.

[58] Smith,P., and Ahmed,A., "Robust Parametrically Varying Attitude Controller Design for the X-33 Vehicle," *AIAA Guidance, Navigation and Control Conference*, AIAA-2000-4158, 2000.

[59] Gahinet,P., Nemirovski,A., Laub,A., and Chilali,M., *LMI Control Toolbox*-Users Guide, The Mathworks,Inc. Natick.,MA,1995.

[60] Jeon,H.,Y., Park,S.,E., Kim, Y., Jun,S., Ku,C.,Y., and Lee,H.,D., "Feasibility Improvement of the Design Space Using Probabilistic Method," *AIAA Aerospace Sciences Meeting and Exhibit*, 2004, AIAA 2004-537.

[61] Hacker,A.,K., Eddy,J., and Lewis,E.,K., "Efficient Global Optimization Using Hybrid Genetic Algorithms," *AIAA/ISSMO Symposium on Multidisciplinary Analysis and Optimization* , 2002, AIAA-2002-5429.

[62] Crespo,G.,L., Daniel P. Giesy,,P.,D., Kenny,P.,S., "Robustness Analysis and Robust Design of Uncertain Systems ," *AIAA Journal*, 2008,Vol. 46, No. 2,pp. 388-396.

BIOGRAPHICAL SKETCH

Sanketh Bhat was born in Mumbai, India in 1984. He did his schooling at O.L.P.S. high school and attended junior college at K.J. Somaiya College of Science. He then attended V.J.T.I. Engineering college affiliated with Mumbai University and graduated with a Bachelor of Engineering (B.E.) degree in June 2006. He did his summer project at CASDE, Department of Aerospace Engineering, Indian Institute of Technology (IIT), Bombay, and worked on the propulsion system of mini aerial vehicles. He also worked as a CFD research engineer at Zeus Numerix Private Limited, Mumbai, India. Sanketh is currently a second-year graduate student in the Department of Mechanical and Aerospace Engineering at the University of Florida. He is studying under Dr. Rick Lind. His research involves control-oriented analysis of hypersonic vehicles. He plans to stay at the University of Florida to pursue a doctoral degree in aerospace engineering with a focus on structural dynamics and control.